Title: Selection on plastic adherence leads to hyper-multicellular strains and incidental virulence in the budding yeast

Luke I. Ekdahl[a,1], Juliana A. Salcedo[a,1], Matthew M. Dungan[a,b], Despina V. Mason[a], Dulguun Myagmarsuren[a], Helen A. Murphy[a,2]

Author Affiliations:
[a]Department of Biology, College of William and Mary, P.O. Box 8795, Williamsburg, VA 23187-8795
[b]Current address: School of Medicine, Vanderbilt University, Nashville, TN 37232
[1]Contributed equally.
[2]To whom correspondence should be addressed.

Helen Murphy
William & Mary
P.O. Box 8795
Williamsburg, VA 23187-8795
757-221-2216
hamurphy@wm.edu

Short Title: Adherence, multicellularity, and virulence in the budding yeast

Key words: yeast, experimental evolution, virulence, adherence, biofilm, *FLO11*

Author Contributions
DVM developed the evolution protocol; JAS evolved the populations; JAS, MMD, LIE, HAM conducted phenotyping; LIE conducted virulence assays; DM prepared genomic samples and analyzed *FLO11* length; HAM conceived of and guided the project, generated the parent strain, analyzed data, and wrote the first draft of the manuscript.

Summary

Many disease-causing microbes are not obligate pathogens; rather, they are environmental microbes taking advantage of an ecological opportunity. The existence of microbes that are not normally pathogenic, yet are well-suited to host exploitation, is an evolutionary paradox. One hypothesis posits that selection in the environment may favor traits that incidentally lead to pathogenicity and virulence, or serve as pre-adaptations for survival in a host. An example of such a trait is surface adherence. To experimentally test the idea of "accidental virulence", replicate populations of the yeast, *Saccharomyces cerevisiae,* which can be an opportunistic pathogen, were evolved to attach to a plastic bead for hundreds of generations. Along with plastic adherence, two multicellular phenotypes— biofilm formation and flor formation— increased; another phenotype, pseudohyphal growth, responded to the nutrient limitation. Thus, experimental selection led to the evolution of highly-adherent, hyper-multicellular strains. Wax moth larvae injected with evolved hyper-multicellular strains were significantly more likely to die than those injected with evolved non-multicellular strains. Hence, selection on plastic adherence incidentally led to the evolution of enhanced multicellularity and increased virulence. Our results support the idea that selection in the environment for a trait unrelated to virulence can inadvertently generate opportunistic, "accidental" pathogens.

1   **Introduction**

2   The study of infectious disease often focuses on pathogenic microbes that either specialize on

3   exploiting animal hosts or on commensals that switch to pathogenesis when the delicate

4   balance between host and microbe is perturbed. These microbes are presumed to have co-

5   evolved complex adaptations that allow survival and reproduction in and on hosts. However,

6   there exists a broad range of microbial organisms that live in the open environment (i.e., soil,

7   vegetation, aquatic habitats) that are capable of causing disease when the opportunity presents

8   itself [1]. Such microbes also have adaptations that allow host exploitation, but the origin of

9   these adaptations is unclear, as growth and survival in a host is not a required part of the

10   lifecycle [2]. For example, the soil-associated bacteria *Pseudomonas aeruginosa* [3] and

11   *Burkholderia cepacia* [4] can infect the lungs of cystic fibrosis patients.

12

13   The 'accidental virulence' hypothesis [2] proposes that adapting to harsh environmental

14   conditions can favor traits that allow certain microbes to be well-suited to exploiting hosts, and

15   challenges the idea that intricate co-evolution is a requirement of microbial pathogenesis and

16   virulence. For example, the fungus *Cryptococcus neoformans* may have 'dual use' virulence

17   factors, such as capsule formation, that are favored in the environment, but that also provide

18   advantages in animal hosts [5]. Other examples include thermotolerance and halotolerance,

19   which may make colonization in and on humans more likely [6,7]. The yeast *Candida auris*,

20   which is found in coastal wetlands, can cause severe systemic infection [8]. One last example is

21   adherence, which is important for many microbial behaviors required for survival (e.g., biofilm

22   formation) [9], but that can also play a role in pathogenicity and virulence [10,11]. In the soil-

23   associated yeast, *Blastomyces dermatitidis* [12], which can cause lung infections, the deletion of

24   a single adhesin gene abolishes pathogenesis [13]. While the function of microbial traits in both

25   the open environment and the host are crucial evidence for the accidental virulence hypothesis,

26   the hypothesis has not been directly tested experimentally.

27

28   To test accidental virulence, we evolved populations of the biomedical model yeast,

29   *Saccharomyces cerevisiae*. Aside from being found in a myriad of ecological niches around the

30   globe [14], *S. cerevisiae* is an opportunistic pathogen capable of infecting immunocompromised

31   individuals, with reports of infections increasing [15–20]. As such, it has been a model for fungal

32   pathogenesis-related traits [21–24]. Some environmentally-derived strains are capable of

33   adhering to surfaces and expressing associated aggregative phenotypes [25]. These range from

34   biofilms on solid and semi-solid agar, to invasive and pseudohyphal growth, to floating mats on

35   liquid surfaces (flors). Of these multicellular phenotypes, only invasive and pseudohyphal

36   growth have been linked to pathogenicity in *S. cerevisiae* [23,24,26], although biofilm formation

37   has been linked to pathogenicity in other fungi [27]. Not all strains are capable of expressing

38   these phenotypes; and while some strains express multiple multicellular traits [28,29], there

39   does not appear to be a correlation among the numerous phenotypes [30]. The ability of a strain

40   to express multicellularity in one form does not necessarily suggest the ability to express it in

41   another, despite overlap in conserved signaling and regulatory networks governing the traits

42   [31]. This is not entirely surprising, since different environmental conditions likely favor different

43   multicellular phenotypes.

44

45   Here, yeast populations were artificially selected for adherence ability in one context, in order to

46   determine whether it led to an increase in virulence in another. Specifically, yeast were evolved

47   to adhere to a plastic bead [32], then tested against wax moth larvae to estimate virulence. In

48   replicate populations of two genetic backgrounds, the yeast increased in their ability to express

49   multicellularity in numerous forms. Not all multicellular phenotypes responded in the same way,

50   with pseudohyphal growth appearing to evolve independently from plastic adherence, biofilm

51   formation and flor formation. This phenotypic evolution demonstrates the complexity of the

52   interacting genetic networks underlying yeast multicellularity. Along with these correlated effects

53   of selection, the yeast also became more virulent. Our results experimentally demonstrate that

54   selection outside of a host environment can inadvertently favor traits that serve as

55   preadaptations for virulence.

56

57   **Results**

58   The evolution experiment was conducted in two genetic backgrounds. While most *S. cerevisiae*

59   strains can be pathogenic against wax moth larvae if administered with a high enough inoculum

60   [24], we chose two strains isolated from clinical settings, and therefore, had a known tendency

61   toward human pathogenicity as well. These strains were highly heterozygous, with tens of

62   thousands of SNPs in each genome [33]; thus, the strains contained standing genetic variation

63   on which selection could act. The first strain, YJM311, was isolated from the bile tube of a

64   patient in San Francisco in 1981 [34]; its recombinant offspring vary in at least one form of

65   filamentous growth [35]. The second strain, YJM128, was isolated from the lung of a patient in

66   Missouri in the 1980's [36]. Both strains were engineered to constitutively express mCherry,

67   then sporulated, digested, and germinated. Each pool of recombinant offspring was used to

68   inoculate replicate populations.

69

70 From each ancestral strain, ten replicate populations were evolved via serial transfer for 350-

71 400 mitotic generations, half punctuated with sexual cycles every 40 generations, and two

72 without beads as controls. YJM311 was

73 evolved for 8 sexual cycles, while YJM128

74 was evolved for 9. Populations were grown

75 in limiting medium in glass tubes in the

76 presence of a plastic bead (Figure 1A-B).

77 After growth, beads were washed,

78 suspended in water, and sonicated to detach

79 cells. The cell suspension was transferred to

80 the next tube for growth (Figure S1). In

81 YJM128, the sexual control failed to

82 propagate after the first cycle. Therefore, a

83 full complement of controls (3 asexual and 3

84 sexual) were subsequently initiated and

85 evolved in the same manner.

86

87 The number of cells attaching to the bead

88 increased over time in the experimental

89 populations (Figure 1; Table S3); thus, the

90 experimental selection protocol had the

91 desired effect. As has been demonstrated in

92 other evolution experiments in

93 microorganisms [37–42], sexual populations

94 showed increased adaptation in comparison

95 to asexual populations (linear mixed-effect

96 model (LMM) with log-transformed bead cell

97 counts: YJM311, asexual*cycle coefficient =

98 0.054 (confidence interval ±0.048),

99 sexual*cycle = 0.184 (±0.048); YJM128,

100 asexual*cycle = 0.47 (±0.242), sexual*cycle

101 = 0.598 (±0.254)).

102
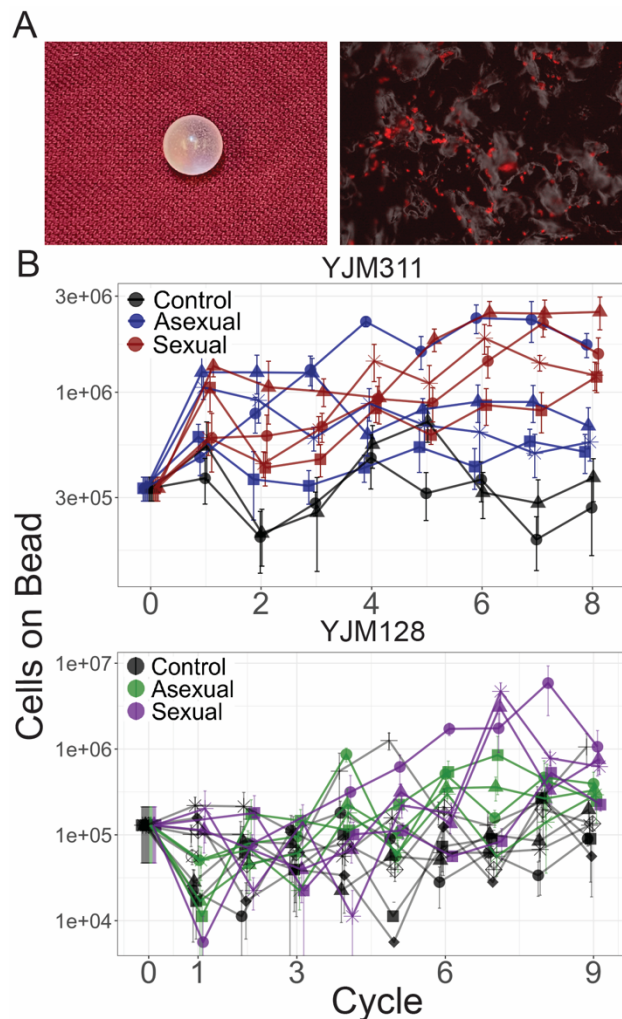
Figure 1: Evolution of bead adherence. (A) Image of a 7mm experimental bead; close-up image with attached cells expressing mCherry. **(B)** Whole population-bead adherence of replicate populations over the experimental cycles. Y-axis plots the number of cells adhering to a plastic bead, as estimated by hemocytometer counts (± S.E.M.) on a log scale. Along with the ancestral timepoint, for each population at each timepoint, cells from 8 replicate beads were counted in YJM311 (670 beads in total); for YJM128, 4 replicate beads were counted (542 beads in total).

103   At the end of the experiment, ten individual clones were isolated from each population from four

104   timepoints (for YJM311, cycles 2, 4, 6, 8, and for YJM128, cycles 1, 3, 6, 9). For each genetic

105   background, over 400 clones, along with 20 ancestral recombinant offspring, were arrayed in a

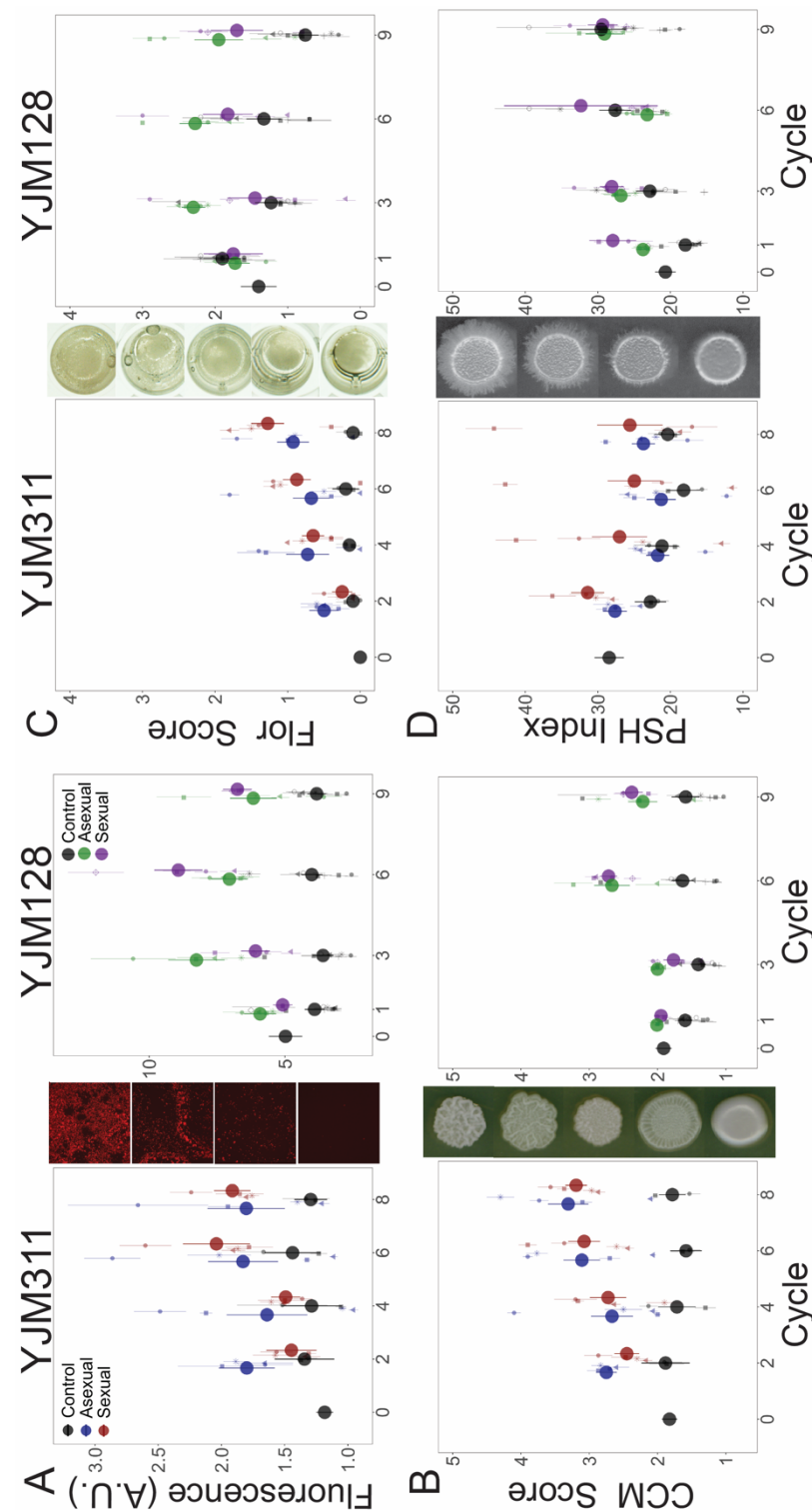106   96-well plate format for analysis of multicellular phenotypes.

Figure 2: Evolution of Multicellular Phenotypes. Ten clones were isolated from each population at four timepoints and assayed in triplicate (except for flor formation, which had a single replicate). In all panels, large points represent the average of a treatment (asexual, sexual, control) ± 2 s.e.m.; smaller points represent the average of a replicate population ± s.e.m. Data at cycle 0 represent the average of 20 ancestral segregants. Representative images demonstrate the variation found in the phenotypes. (A) Plastic adherence was measured using the fluorescence signal of cells remaining in a black, clear-bottom 96-well plate after saturated growth and gentle washing. (B) CCM was scored after growth on solid, glucose-limiting medium using the scale on the right, with 1 representing no biofilm and 5 the most structured colonies. (C) Flor formation was scored after growth in minimal medium using the scale on the right, with 0 representing no floating cells and 4 representing a full mat. (D) PSH was scored after growth on solid nitrogen-limiting medium. Images were processed to determine the percentage of growth pixels that were pseudohyphal compared to the central colony. The trajectory of replicate populations from each ancestral background can be found in Figures S2 and S3.

107　　*Plastic Adherence Ability*

108　　The panel of clones was first assayed for plastic adherence ability (Figure 2A). Plastic

109　　adherence was measured with a microplate reader that detected the fluorescent signal of cells

110　　remaining attached to a well in which culture was grown to saturation and gently rinsed. As

111　　expected, plastic adherence increased over time in the clones from experimental populations

112　　(LMM: YJM311, control*cycle coefficient = 0.008 (confidence interval ±0.056), asexual*cycle =

113　　0.040 (±0.040), sexual*cycle = 0.100 (±0.040); YJM128, control*cycle= 0.016 (±0.076),

114　　asexual*cycle = 0.012 (±0.102); sexual*cycle = 0.187 (±0.114); Table S4). Fluorescent signal

115　　could have evolved over the course of the experiment; indeed, from the beginning, YJM128

116　　produced a brighter fluorescent signal than YJM311, suggesting the existence of genetic

117　　variants that could influence fluorescence expression. Despite the potential for noise in the

118　　measurement, the signal of increased adherence throughout the experiment was apparent in

119　　both genetic backgrounds. These clonal data support the results of the whole-population

120　　adherence measurement (Figure 1), in which cells attaching to a plastic bead were counted

121　　manually with a hemocytometer.

122

123　　We next measured the ability of the clonal panel to express three other seemingly different

124　　multicellular phenotypes.

125

126　　*Biofilm Colony Formation*

127　　The first multicellular phenotype was the ability to form complex colony morphology (CCM) on

128　　solid agar, which is indicative of the ability of a strain to form a differentiated biofilm colony (also

129　　known as a "fluffy colony") [43–47]. This phenotype is correlated with another multicellular

130　　phenotype [30], mat formation, which is a biofilm that forms on semi-solid agar [48]; we

131　　therefore only assayed CCM. Morphology was scored after growth on solid, glucose-limiting

132　　medium using a scale from 1-5, with 1 representing no biofilm and 5 representing the most

133　　structured colonies [30,49] (Figure 2B).

134

135　　In both genetic backgrounds, the selected populations increased in their ability to express CCM

136　　compared to the ancestor (Figure 2B), while the control populations either maintained or

137　　decreased their expression (YJM311: control*cycle coefficient = -0.024 (confidence interval

138　　±0.056), asexual*cycle = 0.119 (±0.039), sexual*cycle = 0.136 (±0.039); YJM128: control*cycle=

139　　0.007 (±0.020), asexual*cycle = 0.048 (±0.026); sexual*cycle = 0.052 (±0.030); Table S5).

140   YJM311 evolved to express stronger CCM than YJM128, despite the latter evolving for one

141   more cycle.

142

143   *Flor Formation*

144   The second multicellular phenotype was the ability to form a flor (or velum), which is a floating

145   mat containing cells attached to one another in an extracellular matrix [29]. Flors form at the

146   liquid-air interface in static conditions and are most commonly found during sherry and wine

147   making processes [50]. Flor formation was scored after growth in minimal medium, with 0

148   representing no floating cells and 4 representing a full mat. The ability to form flors increased in

149   both genetic backgrounds, despite the cultures being grown with agitation (Figure 2C). In

150   YJM311, the ancestral clones showed no ability to generate flors, yet, its evolved populations

151   did (control*cycle coefficient = 0.007 (confidence interval ±0.048), asexual*cycle = 0.075

152   (±0.034), sexual*cycle = 0.163 (±0.034) ; Table S6). In YJM128, ancestral clones showed

153   limited ability to form flors. Its experimental populations either remained or increased in flor-

154   forming ability, while control populations decreased in theirs (control*cycle= -0.109 (±0.032),

155   asexual*cycle = 0.031 (±0.043); sexual*cycle = -0.003 (±0.048) ; Table S6).

156

157   *Pseudohyphal Growth*

158   The final phenotype, pseudohyphal growth (PSH), is a form of filamentous growth thought to

159   represent a foraging strategy. It is characterized by substrate invasion and incomplete

160   separation of mother-daughter cells growing in an elongated, unipolar budding pattern [51]. This

161   phenotype is sometimes correlated with invasive growth, so only PSH was assayed.

162   Filamentous and invasive growth have been associated with pathogenicity and virulence in *S.*

163   *cerevisiae* [23,24,26], as well as in other fungal pathogens of humans and plants [52]. PSH was

164   scored on solid nitrogen-limiting medium; images were processed to determine the percentage

165   of growth that was pseudohyphal compared to the central colony. Unlike the previously assayed

166   phenotypes, the two genetic backgrounds did not evolve similarly with respect to PSH.

167

168   In YJM311, the experimental populations did not increase in their PSH ability compared to the

169   ancestor (Figure 2D); rather, all treatments showed some loss. Throughout the cycles, a

170   moderate level of PSH was maintained in some of the experimental populations, with one

171   sexual replicate doubling its PSH index (Figure S2), but it was lost in the controls and the other

172   experimental populations (control*cycle coefficient = -0.61 (confidence interval ±0.60),

173   asexual*cycle = -0.65 (±0.42), sexual*cycle = -0.97 (±0.43); ; Table S7).

174

175   In YJM128, both the experimental and control populations increased in their PSH ability

176   (control*cycle coefficient = 1.29 (confidence interval $\pm$0.39), asexual*cycle = 0.61 ($\pm$0.51),

177   sexual*cycle = 0.91 ($\pm$0.55) ; Table S7). This was true for the control population that was

178   evolved in concert with all experimental populations, as well as the 6 control populations that

179   were initiated subsequently.

180

181   The results from both ancestral genetic backgrounds suggest that the evolution of PSH was a

182   response to selection in nutrient limiting conditions and not a response to selection for

183   adherence, as the controls and experimental populations behaved similarly. Of all the

184   adherence and multicellular phenotypes investigated, most of which appeared to increase

185   throughout the experiment, PSH appeared to be independent from the others.

186

187   Overall, our phenotyping data show that selection on the ability to adhere to a plastic surface

188   generated a correlated response in multiple multicellular phenotypes, and nutrient limiting

189   conditions favored a further multicellular phenotype in one of the backgrounds.

190

191   *Hyper-multicellularity*

192   To understand the phenotypic landscape of the evolved populations and to determine whether

193   the different forms of multicellularity evolved in concert in individual clones, the clonal phenotype

194   data were combined in a principal components analysis (PCA) (Figure 3A, S4, S5). In YJM311,

195   the loadings of the first two components, which explain 78% of the variation, show that evolved

196   clones with the most extreme values of plastic adherence and flor formation do not tend to also

197   excel at PSH. There were clones, however, that evolved to excel in all of the phenotypes, while

198   not obtaining the most extreme values of the individual traits. In YJM128, the first two loadings

199   explain 70% of the variation, and again, PSH appeared separated from the other multicellular

200   phenotypes. Individual correlations between traits bear out this interpretation (Figure S6, S7).

201   When grouped by experimental treatments, clones from control, asexual, and sexual

202   populations tended to occupy their own, somewhat overlapping, phenotypic space (Figures S4

203   and S5).

204

205   In both backgrounds, as the populations evolved, there were individual clones that increased in

206   all abilities, and became "hyper-multicellular". Thus, a simple process of selection for plastic

207   adherence led to correlated effects in multiple multicellular traits. These correlated effects were

208   apparent both at the population-level, with mean phenotypes increasing in populations over the

209   generations, but also at the individual-level with the evolution of hyper-multicellularity.
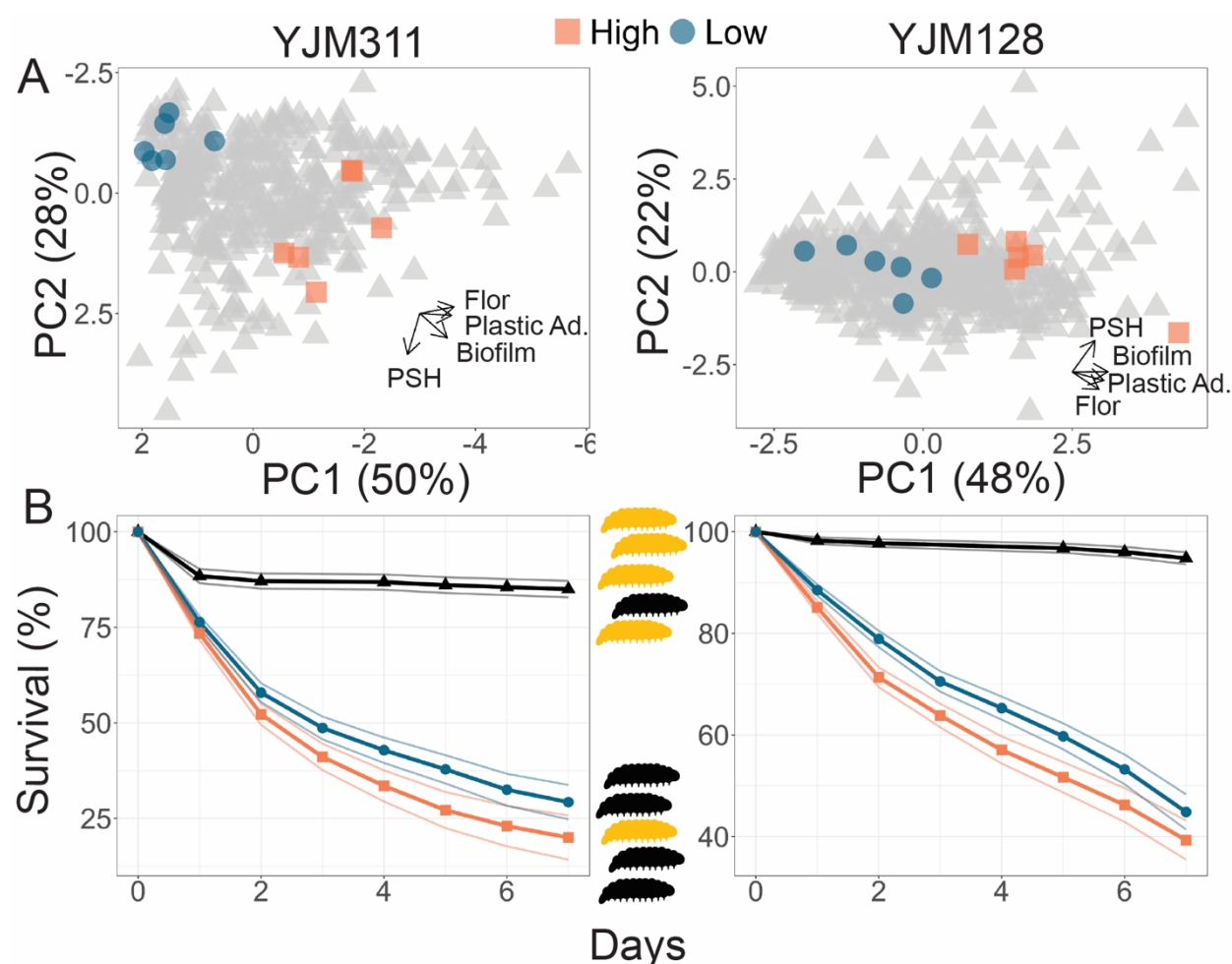
Figure 3: Evolved multicellularity and virulence. (A) Principal components analysis of clones from ancestral and evolved populations. Highlighted points represent strains chosen for virulence assays: blue circles represent low multicellularity clones; orange squares represent hyper-multicellular clones; gray triangles represent the rest of the clonal panel. In YJM311, the non-multicellular clones were chosen from ancestral and control populations, while in YJM128, they were chosen from ancestral and early experimental populations. The loadings of PC1 for YJM311 were -0.616*Flor - 0.573*PA - 0.493*CCM + 0.221*PSH; for PC2, they were 0.851*PSH + 0.506*CCM - 0.137*Flor. In YJM128, the loadings of PC1 were 0.601*CCM + 0.535*PA + 0.451*Flor + 0.386*PSH; for PC2, they were 0.852*PSH - 0.226*PA - 0.472*Flor. PCA with population and cycle information can be found in Figures S4 and S5. **(B)** *G. mellonella* survival curves for strains highlighted in panel A; each strain was injected into 200 larvae for YJM311 derived clones or 180 larvae for YJM128 derived clones. Points represent Kaplan-Meier estimates with confidence limits for non- and hyper-multicellular treatments; black triangles represents the control treatment injected with sterile water. Survival for individual strains is plotted in Figure S10.

210

211   FLO11 *Length Variation*

212   One possible explanation for the increase in multiple forms of multicellularity is a change in a

213   genetic element common to all four phenotypes. A genome-wide investigation into the genetic

214   basis of three multicellular phenotypes (biofilm formation, PSH, and invasive growth) in a lab

215   strain found that each phenotype appeared to have its own set of hundreds of genes underlying

216   its expression, but also some overlap in select

217   transcription factors and signaling pathways

218   [53]. Notably, the one element that all of the

219   traits had in common, as do other aggregative

220   phenotypes, is the requirement of the cell

221   adhesin, Flo11p [48,54,55], which allows yeast

222   cells to adhere to surfaces and other cells [56].

223

224   Flo11p is a cell surface protein with three

225   domains: a C-terminal that facilitates

226   attachment to the cell wall, an exposed N-

227   terminal immunoglobulin-like domain that

228   mediates cell adhesion [57], and a low-

229   complexity, serine-threonine rich B-domain of

230   variable length that extends the adhesion

231   domain away from the cell [56]. The tandem

232   repeats in the B-domain have been shown to

233   be unstable [58,59] and to vary in length

234   naturally [29,60–62] . Differences in the length

235   of this repetitive region have been shown to

236   affect the strength of multicellular phenotypes in

237   some genetic backgrounds [29,59].

238

239   To determine whether *FLO11* length changed

240   throughout the experiment, amplicons of the

Figure 4: *FLO11* length evolution. In 8 ancestral clones and 5 clones per replicate population at the final cycle, the full gene was amplified and run through a BioAnalyzer to determine its length. Amplicons of this length have an accuracy of ±100 bp. x-axis: Anc refers to ancestor, C refers to control populations, A to asexual populations, and S to sexual populations; a-d denote replicates. Top panel: In YJM311, it appears there were two major length alleles, with the possibility of derived variants with smaller changes in length. Bottom panel: In YJM128, it appears there were also two alleles, separated by ~500 bp. Clones from the final timepoint show variation in length.

241   gene were analyzed with electrophoresis in a subset of clones from the final timepoint (Figure

242   4). In the YJM311 populations, five out of eight experimental populations ended with an

243   approximate 1000bp length increase in some or all clones, while none of the control clones

244   showed an increase in length. It is unknown whether the change in length was due to

245   independent *de novo* mutations or selection favoring an existing allele. The similar allelic length

246   in multiple replicate populations favors the latter explanation. It is possible that during the

247   generation of the starting recombinant pool, there was a mutation that was not detected in the

248   subset of ancestral clones later chosen for analysis. In this genetic background, *FLO11* length is

249   not correlated with the strength of plastic adherence, nor with the other three multicellular

250   phenotypes (Figure S8).

251

252   In YJM128, the ancestral pool likely had two alleles separated by a few hundred basepairs. The

253   ending asexual populations appeared to have these alleles, with one much longer allele in a

254   clone in one replicate. The ending sexual populations contained the ancestral alleles, as well as

255   other variants both longer and shorter. Clones from one replicate could not be amplified (Sa),

256   suggesting the possibility of a mutation in the region where the primers anneal. Again, *FLO11*

257   length was not correlated with the strength of plastic adherence, nor with the other three

258   multicellular phenotypes (Figure S9).

259

260   Thus, while *FLO11* length evolved during the experiment, it does not appear to be the cause of

261   the correlated response to selection on adherence. However, this does not rule out the

262   possibility that *FLO11* plays a role. It is possible that expression of the gene, through its

263   complex regulatory network [63–65], is related to the phenotypic response to adherence

264   selection.

265

266   *Virulence*

267   We sought to determine if the evolved changes had an effect on virulence. Virulence was

268   measured using larvae of the greater wax moth, *Galleria mellonella*, an invertebrate model used

269   to study microbial pathogenesis and virulence [66], including in *S. cerevisiae* [67]. Using the

270   PCA results as a guide, for each genetic background, we identified six hyper-multicellular clones

271   from later time points, and six non-multicellular clones from throughout the experiment (Figure

272   3A, Tables S1, S2). Strains were grown in the medium in which they were evolved, then

273   washed, adjusted for density, and injected into larvae. Larval survival and pupation were

274   monitored for the next 7 days. Different batches of larvae can be variable in their response to

275   microbial insult; therefore, to ensure reproducibility of results, the experiment was repeated

276   multiple times with numerous batches of larvae, with each batch being challenged by all strains

277   from a genetic background. For the clones derived from YM311, of the 2400 larvae injected with

278   yeast, 1809 did not survive through day 7. Larvae injected with a hyper-multicellular strain were

279   1.28 times more likely to die than those injected with a non-multicellular strain ($p < 0.001$)

280   (Figures 3B, S10). For the clones derived from YM128, of the 2160 larvae injected with yeast,

281   1113 did not survive through day 7. Larvae injected with a hyper-multicellular strain were 1.29

282   times more likely to die than those injected with a non-multicellular strain (p = 0.032) (Figures

283   4B, S6).

284

285   Thus, the evolutionary changes brought about by selection for adherence to a plastic bead, led

286   to the incidental evolution of increased virulence.

287

288   **Discussion**

289   Our results demonstrate that selection on one yeast trait can generate a correlated response in

290   other traits— a common feature of organismal evolution [68]—, but here, the correlated traits

291   may have included those associated with virulence. In this experiment, favoring the ability to

292   adhere to plastic, a surface that is alarmingly common in industrial, medical, and domestic

293   settings [69], led to a suite of aggregative phenotypes and increased virulence.

294

295   The accidental virulence hypothesis proposes that selection for survival in harsh conditions may

296   lead to traits that predispose microbes to virulence. However, harsh environmental conditions

297   can also favor traits that favor the collective, or multicellular phenotypes [70], so it is perhaps not

298   surprising that other forms of multicellularity increased throughout this experiment. Furthermore,

299   in its long evolutionary history, *S. cerevisiae* has evolved the genetic capability to express

300   multiple different multicellular phenotypes, most of which are induced in nutrient limiting

301   conditions; the experiment presented here was performed in such conditions (glucose limited

302   medium). Other experiments with yeast growing in nutrient limiting conditions have also resulted

303   in the unintended evolution of aggregative behaviors [71]. In this light, the correlated phenotypic

304   responses in this experiment are not entirely unexpected. However, the evolution of *multiple*

305   multicellular phenotypes in *two* independent genetic backgrounds was not anticipated.

306

307   Previous research on a panel of environmental isolates found no correlation between the

308   phenotypes assayed here [30], and in a tractable lab strain capable of aggregative behaviors,

309   each phenotype was associated with its own set of genes [53]. However, there is overlap in the

310   requirement of *FLO11* and its regulators, and despite the fact that the phenotypes are induced

311   by different nutrient signals, there are numerous conserved signaling pathways contributing to

312   filamentous, multicellular growth of all forms (e.g., cAMP-PKA, TOR, filamentous MAPK,

313   Rim101) [31,72]. It is well known that genetic background and genetic architecture can have

314   strong effects on the expression and correlation of traits [73]. In the case of the filamentous

315   phenotypes assayed here, a genetic background that contains variants in the main signaling

316   pathways may lead to a correlation of the phenotypes, while variants expressed later in the

317   development of the phenotype, that are specific to a single trait, may not lead to such a

318   correlation. The effect of the different types of genetic variants suggests that some strains and

319   genetic backgrounds are more likely to evolve virulence from selection in the open environment.

320

321   The strains used in this experiment each contain ~50,000 heterozygous sites and differ from

322   each other by ~25,000 SNPs. It is possible that they contained genetic variation in canonical

323   signaling pathways, allowing for the evolution of hyper-multicellular strains. Interestingly, in both

324   backgrounds, pseudohyphal growth appeared to evolve independently of the other phenotypes.

325   Future research will investigate the sorting of the genetic variation, as well as the new

326   mutations, that led to the observed phenotypic evolution in these populations.

327

328   In our experiment, it is unclear which trait was associated with increased virulence: plastic

329   adherence, a different multicellular trait, general hyper-multicellularity, or an entirely different

330   trait unintentionally favored in the experiment. Regardless of the specific trait causing increased

331   virulence, the experiment demonstrates that selection for a specific trait in an environment that

332   is entirely devoid of host organisms can still inadvertently lead to virulence and pathogenicity.

333

334   The role of environmental opportunistic pathogens in infectious disease is important to consider

335   as humans generate novel ecological niches through the use of plastics, encroach on more

336   habitats, and especially, as the global climate changes [7]. Warmer water temperatures and

337   climate disruptions have been linked to the incidence of illness caused by the marine bacterium

338   *Vibrio vulnificus* [74], and an increase in global temperature has been hypothesized to be

339   related to the simultaneous emergence of *C. auris* infections on multiple continents [75,76].

340   More generally, the narrowing of the gap between mammalian body temperatures and the

341   ambient environment may create opportunities for fungi to exploit new host niches [6]. Thus, as

342   new selective pressures act on existing abundant genetic variation, there is the opportunity to

343   create unintended, accidental pathogens.

344

345   **Materials and Methods**

346   *Strains*

347   To generate strains appropriate for downstream phenotyping assays, the original diploid isolates

348   were was engineered to express a fluorescence protein by fusing mCherry to the C-terminal

349   region of the highly expressed *PGK1* gene, generating HMY7 (YJM311 *PGK1-mCherry-KanMX*)

350   [77] and HMY355 (YJM128 *PGK1-mCherry-HygMX*). After being subject to selection for 8-9

351   cycles, clones with different multicellular phenotypes were isolated from each replicate

352   population (Tables S1-S2).

353

354   *Media*

355   Experimental populations were grown in Evolution Medium (EM; 0.17% yeast nitrogen base

356   without ammonium sulfate and without amino acids, 0.1% glutamic acid, 0.1% dextrose)

357   supplemented with G418 (200 µg/ml) or Hygromycin B (300 µg/ml). Cells were sporulated on

358   solid medium (1% potassium acetate, 2% agar) and digested using an overnight zymolyase- β-

359   glucuronidase procedure [38,78]. Phenotypes were assayed on YPD (1% yeast extract, 2%

360   peptone, 2% dextrose, 2% agar), low dextrose (LD) YPD (0.1% dextrose), 2X SLAD (0.34%

361   yeast nitrogen base without ammonium sulfate and without amino acids, 2% dextrose, 50 µmol

362   ammonium sulfate, 2% agar), or in liquid SD (0.17% yeast nitrogen base without amino acids

363   and with ammonium sulfate, 2% dextrose).

364

365   *Experimental Evolution*

366   HMY7 and HMY355 were grown in 10ml YPD, sporulated, digested, grown to saturation in 10ml

367   EM, and used to inoculate 10 replicate populations: 4 sexual, 4 asexual, and 1 control of each

368   reproductive type.

369

370   Experimental populations derived from YJM311 were evolved for 8 12-day cycles, for a total of

371   ~350 generations; populations from YJM128 were evolved for 9 cycles, for a total of ~400

372   generations. In each cycle, populations were grown in 10ml of EM in a glass tube containing a

373   sterile 7mm polystyrene bead (American Education Products), population size ~ 2 x 10^8. After

374   48 h at 30°C in a rotator drum, the bead was removed with sterile disposable forceps, washed

375   twice, suspended in 500ul of sterile H_2O in a microcentrifuge tube, and gently sonicated

376   (UP200St with VialTweeter, Heischler Ultrasound Technology) to detach cells from the bead.

377   The cell suspension was used to inoculate the next 10ml EM tube. The number of cells on the

378   bead varied over the experiment (Figure 1B). After 4 serial transfers, asexual populations were

379   refrigerated and sexual populations were sporulated for 48 h. Asci were digested overnight, and

380   the spores resuspended in 1ml of EM to allow germination and mating (population size ~ 10^5

381   spores). Finally, the refrigerated cultures and the mated spores were used to begin the next 12-

382   day cycle (Figure S1).

383

384   *Population Phenotyping*

385   To estimate adherence evolution, all populations from all cycles were assayed using the same

386   batch of medium. 10ml EM cultures were inoculated with cryopreserved glycerol stocks and

387   grown for 48 h. From these, two replicate test tubes were inoculated with two beads in each, for

388   a total of four beads per population per time point. The cultures were grown and the beads

389   processed as in the experimental cycle; cell counts were made using a hemocytometer with the

390   sonicated cell suspension. This entire process was repeated a second time, for a total of 8

391   beads per population per cycle for YJM311 populations.

392

393   *Clonal Phenotyping*

394   Twenty clones were isolated from the ancestral population and 10 clones were isolated from

395   each replicate population at four cycle timepoints: 2, 4, 6, 8, for YJM311, and 1, 3, 6, 9, for

396   YJM128. The clonal strains were arrayed in a 96-well format and cryopreserved. To assay

397   social phenotypes, saturated YPD cultures were resuspended and pinned to different media

398   using a 96-pin multi-blot replicator (V&P Scientific no. VP408FP6), wrapped in parafilm, and

399   incubated at 30°C.

400

401   Plastic Adherence: Clones were grown in 200μl EM for 48h in 3 replicate black, clear-bottom,

402   non-treated 96-well plates. Optical density was measured, then culture was removed, and

403   plates were gently washed with water three times and dried upside down for 1h. Fluorescence

404   readings were taken with a Spectramax M2e (Molecular Devices) and used as a proxy for the

405   number of cells that remained attached to the wells. To account for differences in growth, each

406   fluorescence reading was divided by the optical density of the well.

407

408   Flor formation: Clones were grown in 200μl SD for 5d and imaged on an Olympus SZX16

409   dissecting scope. Flor formation was scored using the scale in Figure 2.

410

411 Complex colony morphology (CCM): Clones were pinned to 3 replicate LD omni trays,

412 incubated for 7 days, and imaged on an EPSON Expression 11000 XL scanner. Colonies were

413 scored for complexity using the scale in Figure 2.

414

415 Pseudohyphal growth: Clones were pinned to 3 replicate 2X SLAD omni trays, incubated for 8

416 days, and scanned. Images were processed using a custom script that determined the

417 percentage of colony pixels comprising the pseudohyphae [35].

418

419 Data Analysis

420 Bead cell count data from experimental evolution were log-transformed and analyzed using a

421 mixed effects linear model in R [79] with the lme4 package [80]. Replicate populations within

422 treatments (control, asexual, sexual) was considered a random effect. Because all populations

423 were begun from a single ancestral pool, the intercept was set as the mean value of the

424 ancestor and not allowed to vary among treatments. Therefore, the only fixed effect was the

425 interaction between cycle and treatment, which tested the differences among the slopes of the

426 three treatments. Clonal data were analyzed similarly, with the untransformed average score of

427 a phenotype as the independent variable. Finally, the average phenotyping data for each clone

428 were combined for a principal components analysis in R using the *princomp* function. Figures

429 were produced using ggplot2 [81].

430

431 *Virulence Assay*

432 10ml EM cultures of evolved strains (Table S1) were grown for 48h, washed and resuspended

433 in sterile water to a concentration of 10^9 cells/ml based on hemocytometer counts. 4 µl of culture

434 or control water was injected into the final posterior proleg of *Galleria mellonella* larvae

435 (Vanderhorst Wholesale Inc., https://www.waxworms.net) weighing between 9 and 14 mg using

436 a Hamilton PB600-1 Repeating Dispenser with a 27-gauge needle. Each strain was injected into

437 20 larvae on the same day using the same shipment of *G. mellonella*; 20 control larvae were

438 injected at the start of the assay and at the end. The same assay was repeated the next day

439 with the same shipment of larvae, for a total of 40 larvae/strain/shipment. Multiple shipments

440 were used for the virulence measurements, for a total of 200 larvae per strain for YJM311-

441 derived strains and 160 larvae per strain for YJM128-derived strains. After injection, larvae were

442 incubated at 30°C and survival was monitored for 7 days; larvae that turned black and no longer

443 responded to tactile stimulation were considered dead and removed from the population, as

444 were larvae beginning to pupate.

445

446 Data were analyzed with a mixed effects Cox model using the coxme package [82] in R [79].

447 Death was recorded as the day larvae were removed from the population; larvae were censored

448 if removed for pupation. The model included treatment (high vs. low multicellular) as a fixed

449 effect, and strain and larval batch as random effects.

450

451 *FLO11 Length*

452 Of the clones assayed for multicellular phenotypes, 8 ancestral clones and 5 clones from the

453 final time point of each replicate population were chosen for length analysis. Genomic DNA was

454 extracted using the MasterPure Yeast DNA Purification Kit (Lucigen). *FLO11* was amplified with

455 Phusion polymerase (New England BioLabs) and primers targeting the entire gene (forward:

456 GCC TCA AAA ATC CAT ATA CGC ACA CTA TG, reverse: TTA GAA TAC AAC TGG AAG

457 AGC GAG TAG). Cycle conditions followed manufacturers recommendations and included a

458 melting temperature of 58°C and 3-min extension time. Gene length was estimated by running

459 PCR amplicons through the Agilent 2100 BioAnalyzer using the Agilent DNA 7500 kit (as in ref

460 [60]).

461

462 **Acknowledgements**

467

468

References

1. Brown SP, Cornforth DM, Mideo N. 2012 Evolution of virulence in opportunistic pathogens: generalism, plasticity, and control. *Trends in Microbiology* **20**, 336–342. (doi:10.1016/j.tim.2012.04.005)

2. Casadevall A, Pirofski L. 2007 Accidental virulence, cryptic pathogenesis, martians, lost hosts, and the pathogenicity of environmental microbes. *Eukaryot Cell* **6**, 2169–74. (doi:10.1128/EC.00308-07)

3. Selezska K, Kazmierczak M, Müsken M, Garbe J, Schobert M, Häussler S, Wiehlmann L, Rohde C, Sikorski J. 2012 Pseudomonas aeruginosa population structure revisited under environmental focus: impact of water quality and phage pressure. *Environmental Microbiology* **14**, 1952–1967.

4. Mahenthiralingam E, Baldwin A, Dowson CG. 2008 Burkholderia cepacia complex bacteria: opportunistic pathogens with important natural biology. *Journal of Applied Microbiology* **104**, 1539–51. (doi:10.1111/j.1365-2672.2007.03706.x)

5. Casadevall A, Steenbergen JN, Nosanchuk JD. 2003 'Ready made' virulence and 'dual use' virulence factors in pathogenic environmental fungi — the Cryptococcus neoformans paradigm. *Current Opinion in Microbiology* **6**, 332–337. (doi:10.1016/S1369-5274(03)00082-1)

6. Garcia-Solache Monica A., Casadevall Arturo. In press. Global Warming Will Bring New Fungal Diseases for Mammals. *mBio* **1**, e00061-10. (doi:10.1128/mBio.00061-10)

7. Casadevall A. 2020 Climate change brings the specter of new infectious diseases. *J Clin Invest* **130**, 553–555. (doi:10.1172/JCI135003)

8. Arora Parth *et al.* In press. Environmental Isolation of Candida auris from the Coastal Wetlands of Andaman Islands, India. *mBio* **12**, e03181-20. (doi:10.1128/mBio.03181-20)

9. West SA, Diggle SP, Buckling A, Gardner A, Griffin AS. 2007 The Social Lives of Microbes. *Annual Review of Ecology, Evolution and Systematics* **38**, 53–77. (doi:10.1146/annurev.ecolsys.38.091206.095740)

10. Douglas LJ. 2003 Candida biofilms and their role in infection. *Trends in Microbiology* **11**, 30–36. (doi:10.1016/S0966-842X(02)00002-1)

11. Hall-Stoodley L, Costerton JW, Stoodley P. 2004 Bacterial biofilms: from the natural environment to infectious diseases. *Nature reviews. Microbiology* **2**, 95–108. (doi:10.1038/nrmicro821)

12. Baumgardner DJ, Laundre B. 2001 Studies on the molecular ecology of Blastomyces dermatitidis. *Mycopathologia* **152**, 51–58. (doi:10.1023/A:1012438029997)

13. Klein BS. 2000 Molecular basis of pathogenicity in Blastomyces dermatitidis: the importance of adhesion. *Current Opinion in Microbiology* **3**, 339–343. (doi:10.1016/S1369-5274(00)00100-4)

506   14.   Peter J *et al.* 2018 Genome evolution across 1,011 Saccharomyces cerevisiae isolates.
507   *Nature* **556**, 339–344. (doi:10.1038/s41586-018-0030-5)

508   15.   Aucott JN, Fayen J, Grossnicklas H, Morrissey A, Lederman MM, Salata RA. 1990
509   Invasive infection with Saccharomyces cerevisiae: report of three cases and review. *Reviews*
510   *of infectious diseases* **12**, 406–11.

511   16.   Munoz P, Bouza E, Cuenca-Estrella M, Eiros JM, Perez MJ, Sanchez-Somolinos M,
512   Rincon C, Hortal J, Pelaez T. 2005 Saccharomyces cerevisiae fungemia: an emerging
513   infectious disease. *Clinical infectious diseases : an official publication of the Infectious*
514   *Diseases Society of America* **40**, 1625–34. (doi:10.1086/429916)

515   17.   Llopis S, Hernandez-Haro C, Monteoliva L, Querol A, Molina M, Fernandez-Espinar MT.
516   2014 Pathogenic potential of Saccharomyces strains isolated from dietary supplements. *PloS*
517   *one* **9**, e98094. (doi:10.1371/journal.pone.0098094)

518   18.   Enache-Angoulvant A, Hennequin C. 2005 Invasive Saccharomyces infection: a
519   comprehensive review. *Clinical infectious diseases : an official publication of the Infectious*
520   *Diseases Society of America* **41**, 1559–68. (doi:10.1086/497832)

521   19.   Hennequin C, Kauffmann-Lacroix C, Jobert A, Viard JP, Ricour C, Jacquemin JL,
522   Berche P. 2000 Possible role of catheters in Saccharomyces boulardii fungemia. *European*
523   *journal of clinical microbiology & infectious diseases : official publication of the European*
524   *Society of Clinical Microbiology* **19**, 16–20.

525   20.   Pérez-Torrado R, Querol A. 2016 Opportunistic Strains of Saccharomyces cerevisiae: A
526   Potential Risk Sold in Food Products. *Front Microbiol* **6**, 1522–1522.
527   (doi:10.3389/fmicb.2015.01522)

528   21.   Clemons KV, McCusker JH, Davis RW, Stevens DA. 1994 Comparative pathogenesis of
529   clinical and nonclinical isolates of Saccharomyces cerevisiae. *The Journal of infectious*
530   *diseases* **169**, 859–67.

531   22.   Fraser HB, Levy S, Chavan A, Shah HB, Perez JC, Zhou Y, Siegal ML, Sinha H. 2012
532   Polygenic cis-regulatory adaptation in the evolution of yeast pathogenicity. *Genome research*
533   **22**, 1930–9. (doi:10.1101/gr.134080.111)

534   23.   McCusker JH, Clemons KV, Stevens DA, Davis RW. 1994 Saccharomyces cerevisiae
535   virulence phenotype as determined with CD-1 mice is associated with the ability to grow at 42
536   degrees C and form pseudohyphae. *Infection and immunity* **62**, 5447–55.

537   24.   Phadke, SS, Maclean, CJ, Zhao, SY, Mueller, EA, Michelotti, LA, Norman, KL, Kumar,
538   A, James, TY. 2018 Genome-Wide Screen for Saccharomyces cerevisiae Genes
539   Contributing to Opportunistic Pathogenicity in an Invertebrate Model Host. *G3* , 63–78.
540   (doi:10.1534/g3.117.300245)

541   25.   Verstrepen KJ, Klis FM. 2006 Flocculation, adhesion and biofilm formation in yeasts.
542   *Molecular Microbiology* **60**, 5–15. (doi:10.1111/j.1365-2958.2006.05072.x)
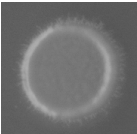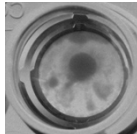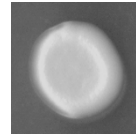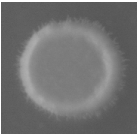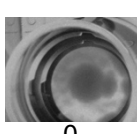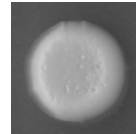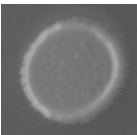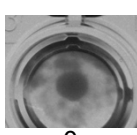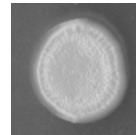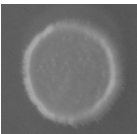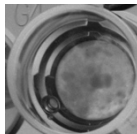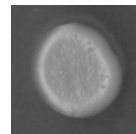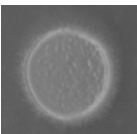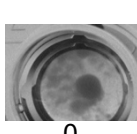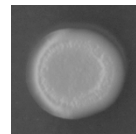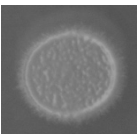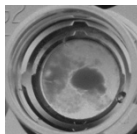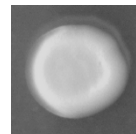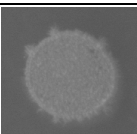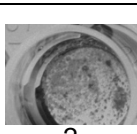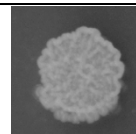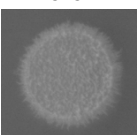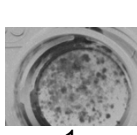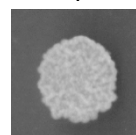
543 26.   Palecek SP, Parikh AS, Kron SJ. 2002 Sensing, signalling and integrating physical
544   processes during Saccharomyces cerevisiae invasive and filamentous growth. *Microbiology*
545   **148**, 893–907. (doi:10.1099/00221287-148-4-893)

546 27.   Fanning S, Mitchell AP. 2012 Fungal Biofilms. *PLoS Pathog* **8**, e1002585.
547   (doi:10.1371/journal.ppat.1002585)

548 28.   Casalone E, Barberio C, Cappellini L, Polsinelli M. 2005 Characterization of
549   Saccharomyces cerevisiae natural populations for pseudohyphal growth and colony
550   morphology. *Research in Microbiology* **156**, 191–200. (doi:10.1016/j.resmic.2004.09.008)

551 29.   Zara G, Zara S, Pinna C, Marceddu S, Budroni M. 2009 FLO11 gene length and
552   transcriptional level affect biofilm-forming ability of wild flor strains of Saccharomyces
553   cerevisiae. *Microbiology (Reading, England)* **155**, 3838–46. (doi:10.1099/mic.0.028738-0)

554 30.   Hope EA, Dunham MJ. 2014 Ploidy-Regulated Variation in Biofilm-Related Phenotypes
555   in Natural Isolates of Saccharomyces cerevisiae. *G3: Genes|Genomes|Genetics* **4**, 1773–
556   1786. (doi:10.1534/g3.114.013250)

557 31.   Cullen PJ, Sprague GF. 2012 The Regulation of Filamentous Growth in Yeast. *Genetics*
558   **190**, 23–49. (doi:10.1534/genetics.111.127456)

559 32.   Traverse CC, Mayo-Smith LM, Poltak SR, Cooper VS. 2013 Tangled bank of
560   experimentally evolved Burkholderia biofilms reflects selection during chronic infections.
561   *Proceedings of the National Academy of Sciences* **110**, E250–E259.
562   (doi:10.1073/pnas.1207025110)

563 33.   Magwene PM, Kayikçi Ö, Granek JA, Reininga JM, Scholl Z, Murray D. 2011
564   Outcrossing, mitotic recombinatino, and life-history trade-offs shape genome evolution in
565   Saccharomyces cerevisiae. *Proceedings of the National Academy of Sciences of the USA*
566   **108**, 1987–1992. (doi:10.1073/pnas.1012544108)

567 34.   McCusker J, Clemons K, Stevens D, Davis R. 1994 Genetic characterization of
568   pathogenic Saccharomyces cerevisiae isolates. *Genetics* **136**, 1261–9.

569 35.   Lenhart BA, Meeks B, Murphy HA. 2019 Variation in Filamentous Growth and Response
570   to Quorum-Sensing Compounds in Environmental Isolates of Saccharomyces cerevisiae. *G3:*
571   *Genes|Genomes|Genetics* **9**, 1533. (doi:10.1534/g3.119.400080)

572 36.   Tawfik OW, Papasian CJ, Dixon AY, Potter LM. 1989 Saccharomyces cerevisiae
573   pneumonia in a patient with acquired immune deficiency syndrome. *Journal of Clinical*
574   *Microbiology* **27**, 1689–1691.

575 37.   Zeyl C, Bell G. 1997 The advantage of sex in evolving yeast populations. *Nature* **388**,
576   465–468.

577 38.   Goddard M, Godfray C, Burt A. 2005 Sex increases the efficacy of natural selection in
578   experimental yeast populations. *Nature* **434**, 636–640.

579 39.   McDonald MJ, Rice DP, Desai MM. 2016 Sex speeds adaptation by altering the
580   dynamics of molecular evolution. *Nature* **531**, 233–236. (doi:10.1038/nature17143)

581   40.   Kosheleva K, Desai MM. 2018 Recombination Alters the Dynamics of Adaptation on
582   Standing Variation in Laboratory Yeast Populations. *Molecular Biology and Evolution* **35**,
583   180–201. (doi:10.1093/molbev/msx278)

584   41.   Kaltz O, Bell G. 2002 The ecology and genetics of fitness in Chlamydomonas. XII.
585   Repeated sexual episodes increase rates of adaptation to novel environments. *Evolution* **56**,
586   1743–53. (doi:doi: 10.1111/j.0014-3820.2002.tb00188.x)

587   42.   Lachapelle J, Bell G. 2012 Evolutionary rescue of sexual and asexual populations in a
588   deteriorating environment. *Evolution* **66**, 3508–18. (doi:doi: 10.1111/j.1558-
589   5646.2012.01697.x)

590   43.   Kuthan M, Devaux F, Janderová B, Slaninová I, Jacq C, Palková Z. 2003 Domestication
591   of wild Saccharomyces cerevisiae is accomplanied by changes in gene expression and
592   colony morphology. *Molecular Microbiology* **47**, 745–754.

593   44.   Štovíček V, Váchová L, Kuthan M, Palková Z. 2010 General factors important for the
594   formation of structured biofilm-like yeast colonies. *Fungal Genetics and Biology* **47**, 1012–
595   1022. (doi:10.1016/j.fgb.2010.08.005)

596   45.   Sťovicek V, Vachova L, Begany M, Wilkinson D, Palkova Z. 2014 Global changes in
597   gene expression associated with phenotypic switching of wild yeast. *Bmc Genomics* **15**.
598   (doi:10.1186/1471-2164-15-136)

599   46.   Váchová L, Šťovíček V, Hlaváček O, Chernyavskiy O, Štěpánek L, Kubínová L, Palková
600   Z. 2011 Flo11p, drug efflux pumps, and the extracellular matrix cooperate to form biofilm
601   yeast colonies. *The Journal of Cell Biology* **194**, 679–687. (doi:10.1083/jcb.201103129)

602   47.   Maršíková J *et al.* 2017 Metabolic differentiation of surface and invasive cells of yeast
603   colony biofilms revealed by gene expression profiling. *BMC Genomics* **18**, 814.
604   (doi:10.1186/s12864-017-4214-4)

605   48.   Reynolds TB, Fink GR. 2001 Bakers' Yeast, a Model for Fungal Biofilm Formation.
606   *Science* **291**, 878–881. (doi:10.1126/science.291.5505.878)

607   49.   Granek JA, Magwene PM. 2010 Environmental and Genetic Determinants of Colony
608   Morphology in Yeast. *PLoS Genet* **6**, e1000823.

609   50.   Legras J-L *et al.* 2016 Flor Yeast: New Perspectives Beyond Wine Aging. *Frontiers in
610   Microbiology* **7**.

611   51.   Gimeno CJ, Ljungdahl PO, Styles CA, Fink GR. 1992 Unipolar cell divisions in the yeast
612   S. cerevisiae lead to filamentous growth: regulation by starvation and RAS. *Cell* **68**, 1077–90.

613   52.   Lengeler KB, Davidson RC, D'souza C, Harashima T, Shen W-C, Wang P, Pan X,
614   Waugh M, Heitman J. 2000 Signal transduction cascades regulating fungal development and
615   virulence. *Microbiology and molecular biology reviews* **64**, 746–785.

616   53.   Ryan O *et al.* 2012 Global gene deletion analysis exploring yeast filamentous growth.
617   *Science (New York, N.Y.)* **337**, 1353–6. (doi:10.1126/science.1224339)

618   54.   Zara S, Bakalinsky AT, Zara G, Pirino G, Demontis MA, Budroni M. 2005 FLO11-based
619   model for air-liquid interfacial biofilm formation by Saccharomyces cerevisiae. *Appl Environ*
620   *Microbiol* **71**, 2934–2939. (doi:10.1128/AEM.71.6.2934-2939.2005)

621   55.   Lo W-S, Dranginis AM. 1998 The Cell Surface Flocculin Flo11 Is Required for
622   Pseudohyphae Formation and Invasion by Saccharomyces cerevisiae. *Molecular Biology of*
623   *the Cell* **9**, 161–171. (doi:10.1091/mbc.9.1.161)

624   56.   Dranginis AM, Rauceo JM, Coronado JE, Lipke PN. 2007 A biochemical guide to yeast
625   adhesins: glycoproteins for social and antisocial occasions. *Microbiology and molecular*
626   *biology reviews : MMBR* **71**, 282–94. (doi:10.1128/mmbr.00037-06)

627   57.   Kraushaar T, Brückner S, Veelders M, Rhinow D, Schreiner F, Birke R, Pagenstecher A,
628   Mösch H-U, Essen L-O. 2015 Interactions by the Fungal Flo11 Adhesin Depend on a
629   Fibronectin Type III-like Adhesin Domain Girdled by Aromatic Bands. *Structure* **23**, 1005–
630   1017. (doi:10.1016/j.str.2015.03.021)

631   58.   Fidalgo M, Barrales RR, Ibeas JI, Jimenez J. 2006 Adaptive evolution by mutations in
632   the FLO11 gene. *Proceedings of the National Academy of Sciences of the United States of*
633   *America* **103**, 11228–33. (doi:10.1073/pnas.0601713103)

634   59.   Fidalgo M, Barrales RR, Jimenez J. 2008 Coding repeat instability in the FLO11 gene of
635   Saccharomyces yeasts. *Yeast (Chichester, England)* **25**, 879–89. (doi:10.1002/yea.1642)

636   60.   Oppler ZJ, Parrish ME, Murphy HA. 2019 Variation at an adhesin locus suggests the
637   possibility of self-discrimination in the yeast Saccharomyces cerevisiae. *Proceedings of the*
638   *Royal Society B-Biological Sciences* **286**, 20191948. (doi:10.1098/rspb.2019.1948)

639   61.   David-Vaizant V, Alexandre H. 2018 Flor Yeast Diversity and Dynamics in Biologically
640   Aged Wines. *Frontiers in Microbiology* **9**. (doi:10.3389/fmicb.2018.02235)

641   62.   Verstrepen KJ, Jansen A, Lewitter F, Fink GR. 2005 Intragenic tandem repeats generate
642   functional variability. *Nature genetics* **37**, 986–90. (doi:10.1038/ng1618)

643   63.   Rupp S, Summers E, Lo HJ, Madhani H, Fink G. 1999 MAP kinase and cAMP
644   filamentation signaling pathways converge on the unusually large promoter of the yeast
645   FLO11 gene. *Embo Journal* **18**, 1257–1269. (doi:10.1093/emboj/18.5.1257)

646   64.   Octavio LM, Gedeon K, Maheshri N. 2009 Epigenetic and Conventional Regulation Is
647   Distributed among Activators of FLO11 Allowing Tuning of Population-Level Heterogeneity in
648   Its Expression. *PLOS Genetics* **5**, e1000673. (doi:10.1371/journal.pgen.1000673)

649   65.   Bumgarner SL, Dowell RD, Grisafi P, Gifford DK, Fink GR. 2009 Toggle involving cis-
650   interfering noncoding RNAs controls variegated gene expression in yeast. *Proceedings of the*
651   *National Academy of Sciences of the United States of America* **106**, 18321–6.
652   (doi:10.1073/pnas.0909641106)

653   66.   Pereira TC, De Barros PP, Fugisaki LR, Rossoni RD, Ribeiro FD, De Menezes RT,
654   Junqueira JC, Scorzoni L. 2018 Recent Advances in the Use of Galleria mellonella Model to
655   Study Immune Responses against Human Pathogens. *Journal of Fungi* **4**.
656   (doi:10.3390/jof4040128)

67. Phadke SS, Maclean CJ, Zhao SY, Mueller EA, Michelotti LA, Norman KL, Kumar A, James TY. 2018 Genome-Wide Screen for Saccharomyces cerevisiae Genes Contributing to Opportunistic Pathogenicity in an Invertebrate Model Host. *G3 Genes|Genomes|Genetics* **8**, 63–78. (doi:10.1534/g3.117.300245)

68. Price T, Langen T. 1992 Evolution of correlated characters. *Trends in Ecology & Evolution* **7**, 307–310. (doi:10.1016/0169-5347(92)90229-5)

69. Geyer Roland, Jambeck Jenna R., Law Kara Lavender. In press. Production, use, and fate of all plastics ever made. *Science Advances* **3**, e1700782. (doi:10.1126/sciadv.1700782)

70. Tong K, Bozdag GO, Ratcliff WC. 2022 Selective drivers of simple multicellularity. *Current Opinion in Microbiology* **67**, 102141. (doi:10.1016/j.mib.2022.102141)

71. Hope EA, Amorosi CJ, Miller AW, Dang K, Heil CS, Dunham MJ. 2017 Experimental Evolution Reveals Favored Adaptive Routes to Cell Aggregation in Yeast. *Genetics* **206**, 1153–1167. (doi:10.1534/genetics.116.198895)

72. Granek JA, Kayikçi Ö, Magwene PM. 2011 Pleiotropic signaling pathways orchestrate yeast development. *Current Opinion in Microbiology* **14**, 676–681. (doi:10.1016/j.mib.2011.09.004)

73. Gasch AP, Payseur BA, Pool JE. 2016 The power of natural variation for model organism biology. *Trends in Genetics* **32**, 146–154.

74. Martinez-Urtaza J, Bowers JC, Trinanes J, DePaola A. 2010 Climate anomalies and the increasing risk of Vibrio parahaemolyticus and Vibrio vulnificus illnesses. *Food Research International* **43**, 1780–1790. (doi:10.1016/j.foodres.2010.04.001)

75. Jackson BR, Chow N, Forsberg K, Litvintseva AP, Lockhart SR, Welsh R, Vallabhaneni S, Chiller T. 2019 On the Origins of a Species: What Might Explain the Rise of Candida auris? *Journal of Fungi* **5**. (doi:10.3390/jof5030058)

76. Sharma Megha, Chakrabarti Arunaloke, Hube Bernhard, Hube Bernhard. In press. On the Origin of Candida auris: Ancestor, Environmental Stresses, and Antiseptics. *mBio* **11**, e02102-20. (doi:10.1128/mBio.02102-20)

77. Deschaine BM, Heysel AR, Lenhart BA, Murphy HA. 2018 Biofilm formation and toxin production provide a fitness advantage in mixed colonies of environmental yeast isolates. *Ecology and Evolution* **8**, 5541–5550. (doi:10.1002/ece3.4082)

78. Granek JA, Murray D, Kayikçi Ö, Magwene PM. 2013 The Genetic Architecture of Biofilm Formation in a Clinical Isolate of Saccharomyces cerevisiae. *Genetics* **193**, 587–600. (doi:10.1534/genetics.112.142067)

79. Team RC. 2020 *R: A language and environment for statistical computing.* Vienna, Austria. See https://www.R-project.org/.

80. Bates D, Maechler M, Bolker B, Walker S. 2015 Fitting Linear Mixed-Effects Models Using lme4. *Journal of Statistical Software* **67**, 1–48. (doi:10.18637/jss.v067.i01)

694   81.   Wickham H. 2016 *ggplot2: Elegant Graphics for Data Analysis*. New York: Springer-
695   Verlag.

696   82.   Therneau TM. 2020 *coxme: Mixed Effects Cox Models*. See https://CRAN.R-
697   project.org/package=coxme.

698

699
700

Strain Name	Background (RepPop-Cycle-Clone#)	Experimental Identity	Multicellular Designation	Avg. PSH Index	Avg. Flor Score	Avg. CCM Score	Avg. Fluor. Read.
HMY7	YJM311, *PGK1-mCherry-KanMX*	Ancestor	Heterozygous Ancestral Isolate				
HMY596	C7s-8-8	Sexual control clone (cycle 8)	Low (L1)	26.33	0	1	1.174
HMY597	Anc-0-3	Ancestral clone	Low (L2)	24.5	0	1	0.939
HMY598	C7a-8-6	Asexual control clone (cycle 8)	Low (L3)	16	0	2	1.573
HMY599	C7s-8-5	Sexual control clone (cycle 8)	Low (L4)	18.33	0	1	1.204
HMY600	C7a-2-10	Asexual control clone (cycle 2)	Low (L5)	16	0	1	1.233
HMY601	C7s-2-1	Sexual control clone (cycle 2)	Low (L6)	26	0	1	1.475
HMY602	A7b-8-9	Asexual experimental clone (cycle 8)	High (H1)	26.67	2	4	2.082
HMY603	A7a-8-3	Asexual experimental clone (cycle 8)	High (H2)	31.33	1	4	1.454
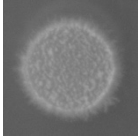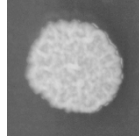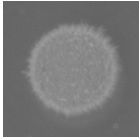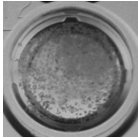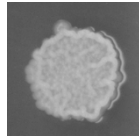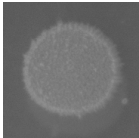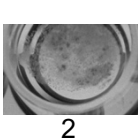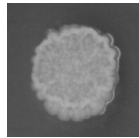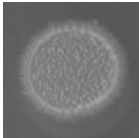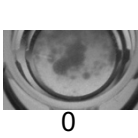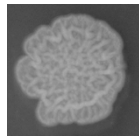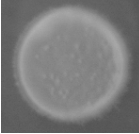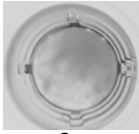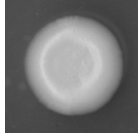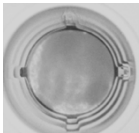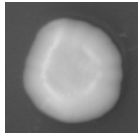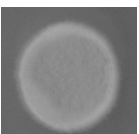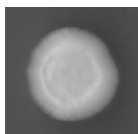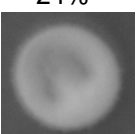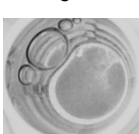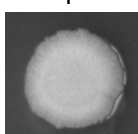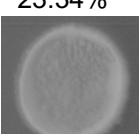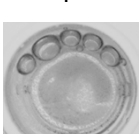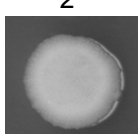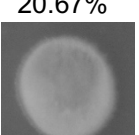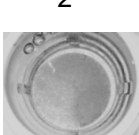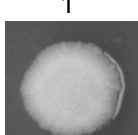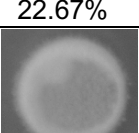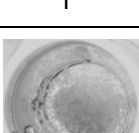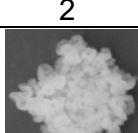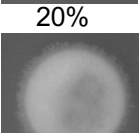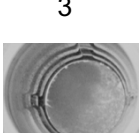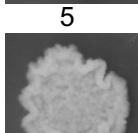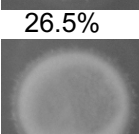
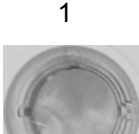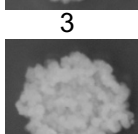|							
HMY604	S7d-8-1	Sexual experimental clone (cycle 8)	High (H3)	38.5	1	4	2.095
HMY605	S7b-8-8	Sexual experimental clone (cycle 8)	High (H4)	20.5	2	3	1.925
HMY606	S7a-8-9	Sexual experimental clone (cycle 8)	High (H5)	18.5	2	3.33	1.599
HMY607	A7d-8-3	Asexual experimental clone (cycle 8)	High (H6)	22.67	0	5	1.259

701 **Table S1: YJM311 Strains used in virulence experiments.**
702

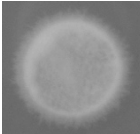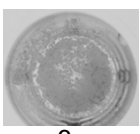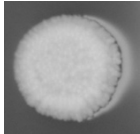| Strain Name	Background (RepPop-Cycle-Clone#)	Experimental Identity	Multicellular Designation	Avg. PSH Index	Avg. Flor Score	Avg. CCM Score	Avg. Fluor. Read.
HMY355	YJM128, *PGK1-mCherry-HygMX*	Ancestor	Heterozygous Ancestral Isolate				
HMY580	S8d-3-6	Sexual experimental clone (cycle 3)	Low (L1)	26%	0	1	6.04
HMY581	S8b-1-10	Sexual experimental clone (cycle 1)	Low (L2)	22%	0	1	3.44
HMY582	S8b-3-8	Sexual experimental clone (cycle 3)	Low (L3)	24%	0	1	8.78
HMY579	Anc-8-5	Ancestral clone	Low (L4)	23.34%	1	2	4.66
HMY584	A8c-3-10	Asexual control clone (cycle 3)	Low (L5)	20.67%	2	1	7.5
HMY575	Anc-8-19	Ancestral clone	Low (L6)	22.67%	1	2	7.3
HMY570	A8a-6-8	Asexual experimental clone (cycle 6)	High (H1)	20%	3	5	11.06
HMY571	S8b-6-1	Sexual experimental clone (cycle 6)	High (H2)	26.5%	1	3	9.04
HMY572	A8d-9-10	Asexual experimental clone (cycle 9)	High (H3)	29.67%	0	3.34	9.23
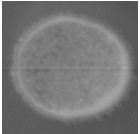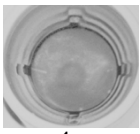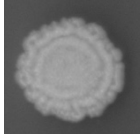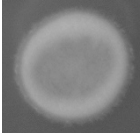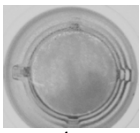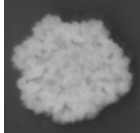
HMY573	S8b-9-5	Sexual experimental clone (cycle 9)	High (H4)	31.67%	1	2.34	6.93
HMY574	A8d-9-2	Asexual experimental clone (cycle 9)	High (H5)	27.33%	1	3.67	6.34
HMY576	A8a-9-8	Asexual experimental clone (cycle 9)	High (H6)	39%	3	2	7.79

703
704

Table S2: YJM128 Strains used in virulence experiments.

705

	YJM311			YJM128		
Fixed Effects	coefficient	st. error	t-value	coefficient	st. error	t-value
Cycle: Control	-0.05528	0.03437	-1.608	0.02182	0.09041	0.241
Cycle: Sexual	**0.05407**	0.02433	2.223	**0.46993**	0.12151	3.868
Cycle: Asexual	**0.18435**	0.02422	7.612	**0.59841**	0.12747	4.695
Random Effects	variance			variance		
Population(Treatment)	0.2593			7.683		
Residual	0.9466			17.302		
Residual DF	629			525		

706
707 **Table S3: Results of the mixed-effect linear model for whole-population cell count data over
708 experimental cycles.** Cell counts were transformed by adding one and taking the natural log; data were
709 analyzed with the lme4 package in R. Coefficients whose confidence intervals do not encompass zero
710 are bolded.
711
712
713

	YJM311			YJM128		
Fixed Effects	coefficient	st. error	t-value	coefficient	st. error	t-value
Cycle: Control	0.008143	0.028509	0.286	0.01614	0.03805	0.424
Cycle: Sexual	0.039812	0.020266	1.964	0.01174	0.05184	0.227
Cycle: Asexual	**0.100228**	0.020125	4.980	**0.18686**	0.05661	3.301
Random Effects	variance			variance		
Population(Treatment)	0.1482			2.328		
Residual	0.4347			4.066		
Residual DF	391			574		

714
715 **Table S4: Results of the mixed-effect linear model for clonal plastic adherence data.** Data were
716 analyzed with the lme4 package in R. Coefficients whose confidence intervals do not encompass zero
717 are bolded.
718
719
720
721

	YJM311			YJM128		
Fixed Effects	coefficient	st. error	t-value	coefficient	st. error	t-value
Cycle: Control	-0.02432	0.02783	-0.874	0.007192	0.009940	0.724
Cycle: Sexual	**0.11899**	0.01968	6.046	**0.048360**	0.013161	3.675
Cycle: Asexual	**0.13610**	0.01968	6.916	**0.052230**	0.014772	3.536
Random Effects	variance			variance		
Population(Treatment)	0.2748			0.1702		
Residual	0.3588			0.2789		
Residual DF	395			584		

722
723 **Table S5: Results of the mixed-effect linear model for clonal CCM data.** Data were analyzed with the
724 lme4 package in R. Coefficients whose confidence intervals do not encompass zero are bolded.
725
726
727

Fixed Effects	YJM311			YJM128		
	coefficient	st. error	t-value	coefficient	st. error	t-value
Cycle: Control	0.006646	0.024077	0.276	**-0.10927**	0.01633	-6.692
Cycle: Sexual	**0.074519**	0.017025	4.377	0.03118	0.02161	1.443
Cycle: Asexual	**0.162927**	0.017025	9.570	-0.00291	0.02407	-0.121
Random Effects	variance			variance		
Population(Treatment)	0.1678			0.3527		
Residual	0.2780			0.7740		
Residual DF	395			584		

728
729 **Table S6: Results of the mixed-effect linear model for clonal flor data.** Data were analyzed with the
730 lme4 package in R. Coefficients whose confidence intervals do not encompass zero are bolded.
731
732
733
734
735

Fixed Effects	YJM311			YJM128		
	coefficient	st. error	t-value	coefficient	st. error	t-value
Cycle: Control	**-0.6111**	0.3012	-2.029	**1.2908**	0.1952	6.612
Cycle: Sexual	**-0.6474**	0.2130	-3.040	**0.6096**	0.2572	2.370
Cycle: Asexual	**-0.9649**	0.2156	-4.475	**0.9085**	0.2750	3.304
Random Effects	variance			variance		
Population(Treatment)	44.81			21.48		
Residual	40.29			126.08		
Residual DF	390			584		

736
737 **Table S7: Results of the mixed-effect linear model for clonal PSH data.** Data were analyzed with the
738 lme4 package in R. Coefficients whose confidence intervals do not encompass zero are bolded.
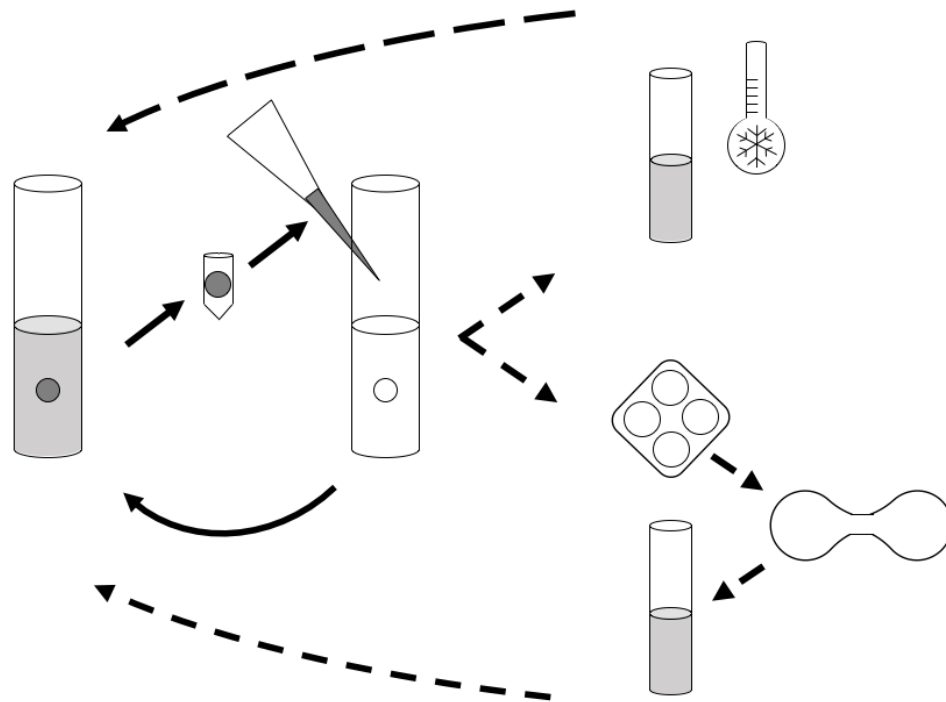739
740
741
742
743

744 **Figure S1: Schematic of the Experimental Cycle.** Solid arrows represent steps in serial
745 transfer; dashed lines represent punctuated sexual treatments. Populations were evolved on a
746 12-day cycle. In each cycle, populations were grown in 10ml of minimal medium in a glass tube
747 containing a sterile 7mm polystyrene bead for 48 h with rotation. The bead was removed,
748 washed, suspended in water, and gently sonicated to detach cells from the bead. The cell
749 suspension was used to inoculate the next 10ml tube. After 4 serial transfers, asexual
750 populations were refrigerated and sexual populations were sporulated for 48 h. Asci were
751 digested, germinated and mated. Refrigerated cultures and mated spores were used to begin
752 the next 12-day cycle.
753
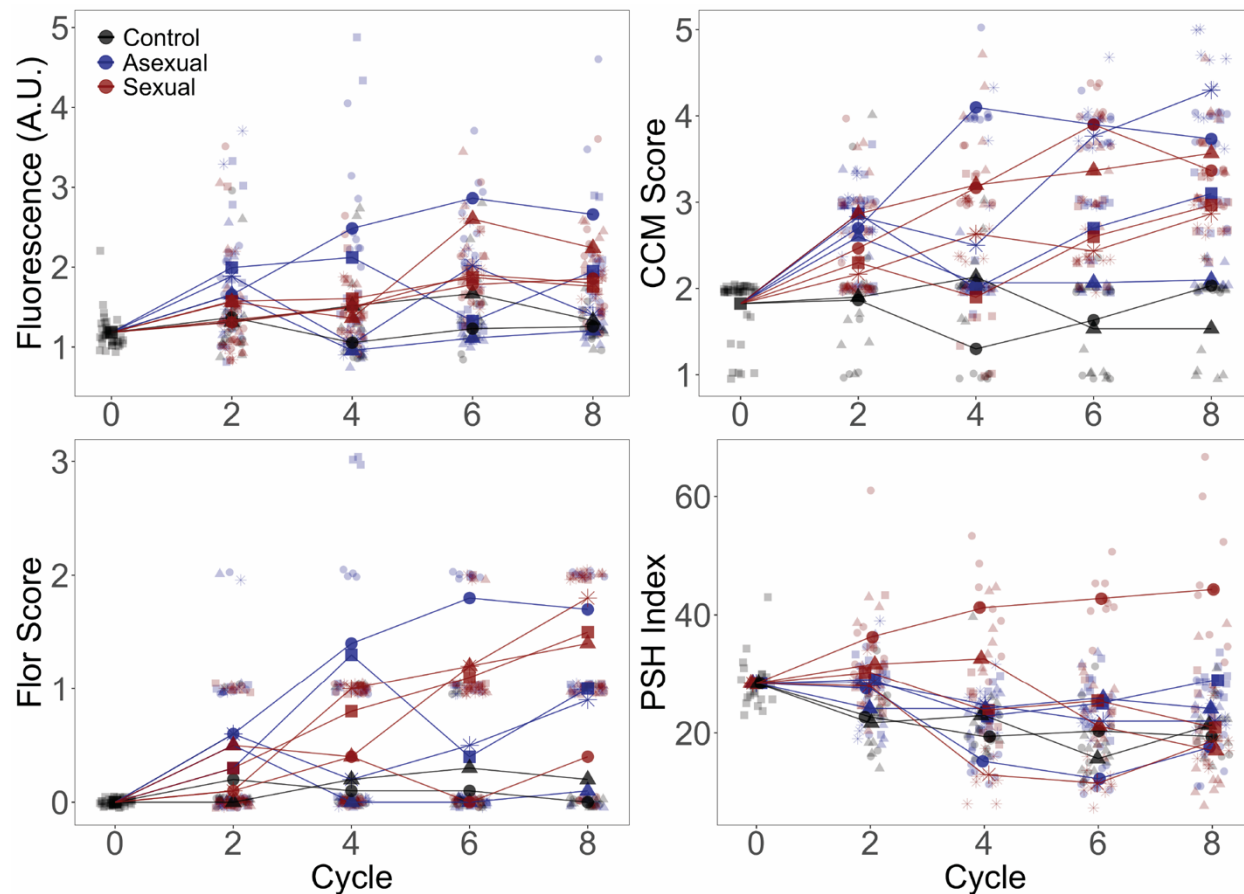
Figure S2: Evolved Phenotypes by Replicate Population for the YJM311 Background. Phenotypes were assessed as in Figure 2. Larger points represent replicate population averages, with each replicate represented by a different shape/color combination (as in Figure 4); smaller points represent measurements from individual clones. Fluorescence, CCM, and PSH are average values of three replicate measurements per clone; Flor is based on one replicate.
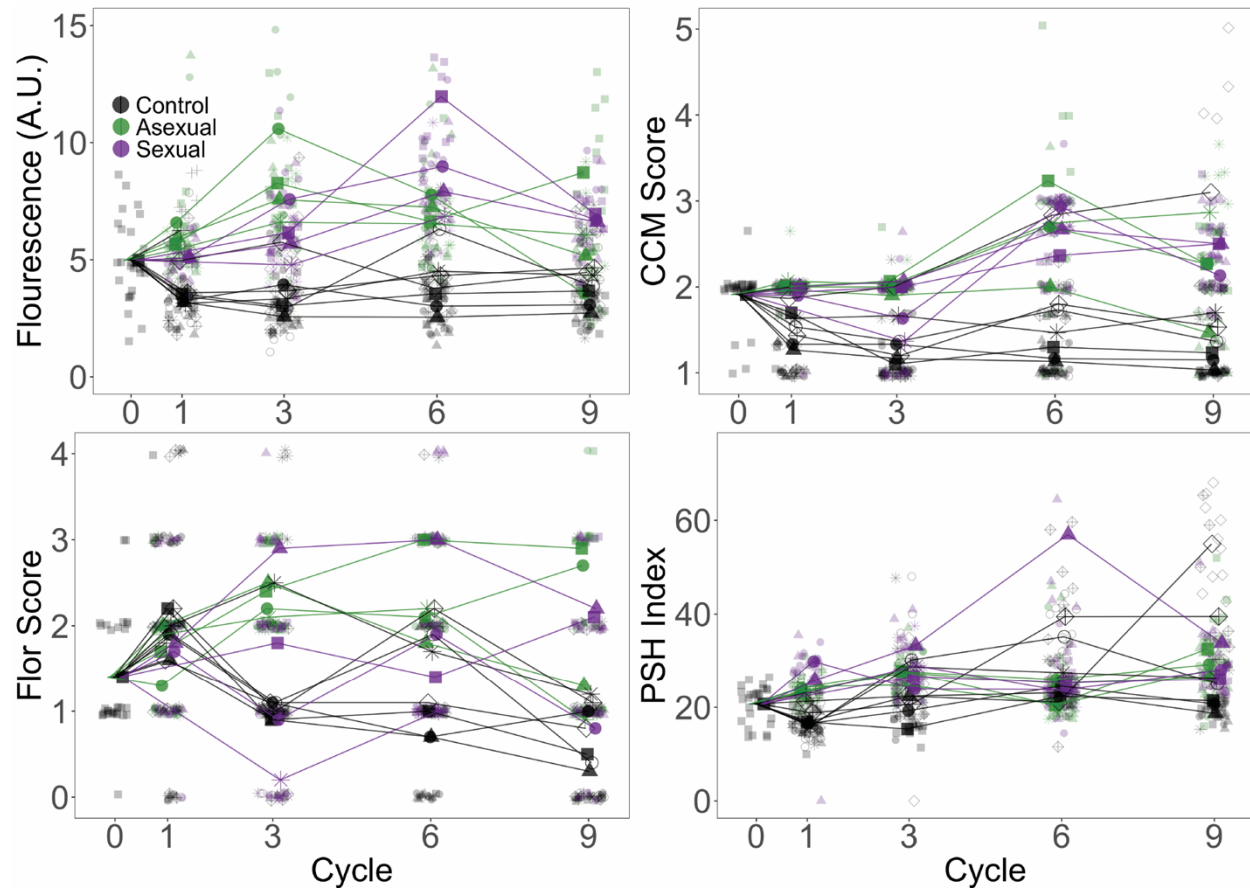
Figure S3: Evolved Phenotypes by Replicate Population for the YJM128 Background. Phenotypes were assessed as in Figure 2. Larger points represent replicate population averages, with each replicate represented by a different shape/color combination (as in Figure 4); smaller points represent measurements from individual clones. Fluorescence, CCM, and PSH are average values of three replicate measurements per clone; Flor is based on one replicate.
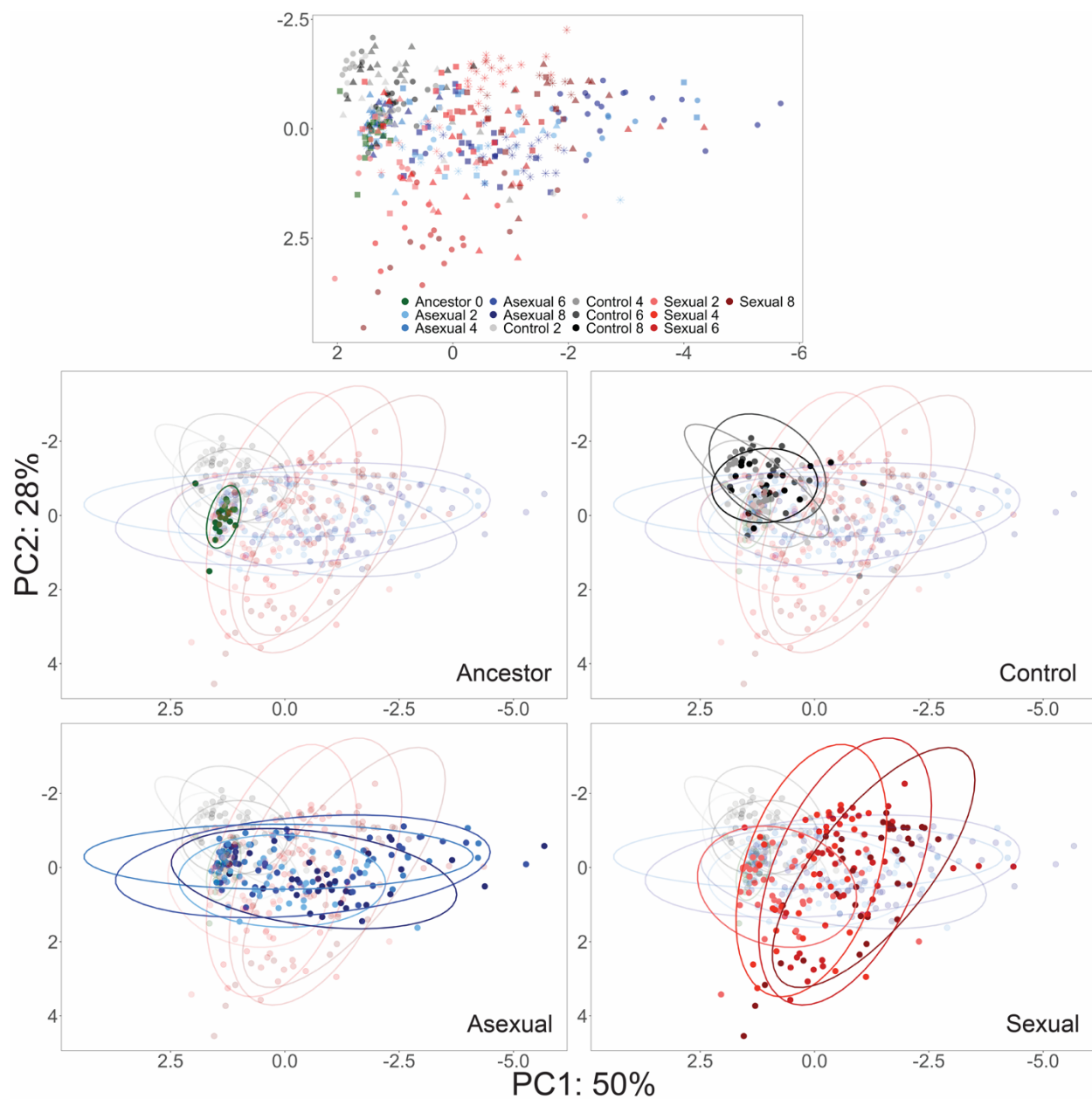
769
770 **Figure S4: PCA of YJM311 Evolved Populations.**
771 Each point represents a single clone; ancestor- green, control- gray through black, asexual- light
772 blue through dark blue, sexual- light red through dark red. Colors become darker as cycle
773 number increases. In the first panel, shapes as in Figure 4 to highlight different replicate
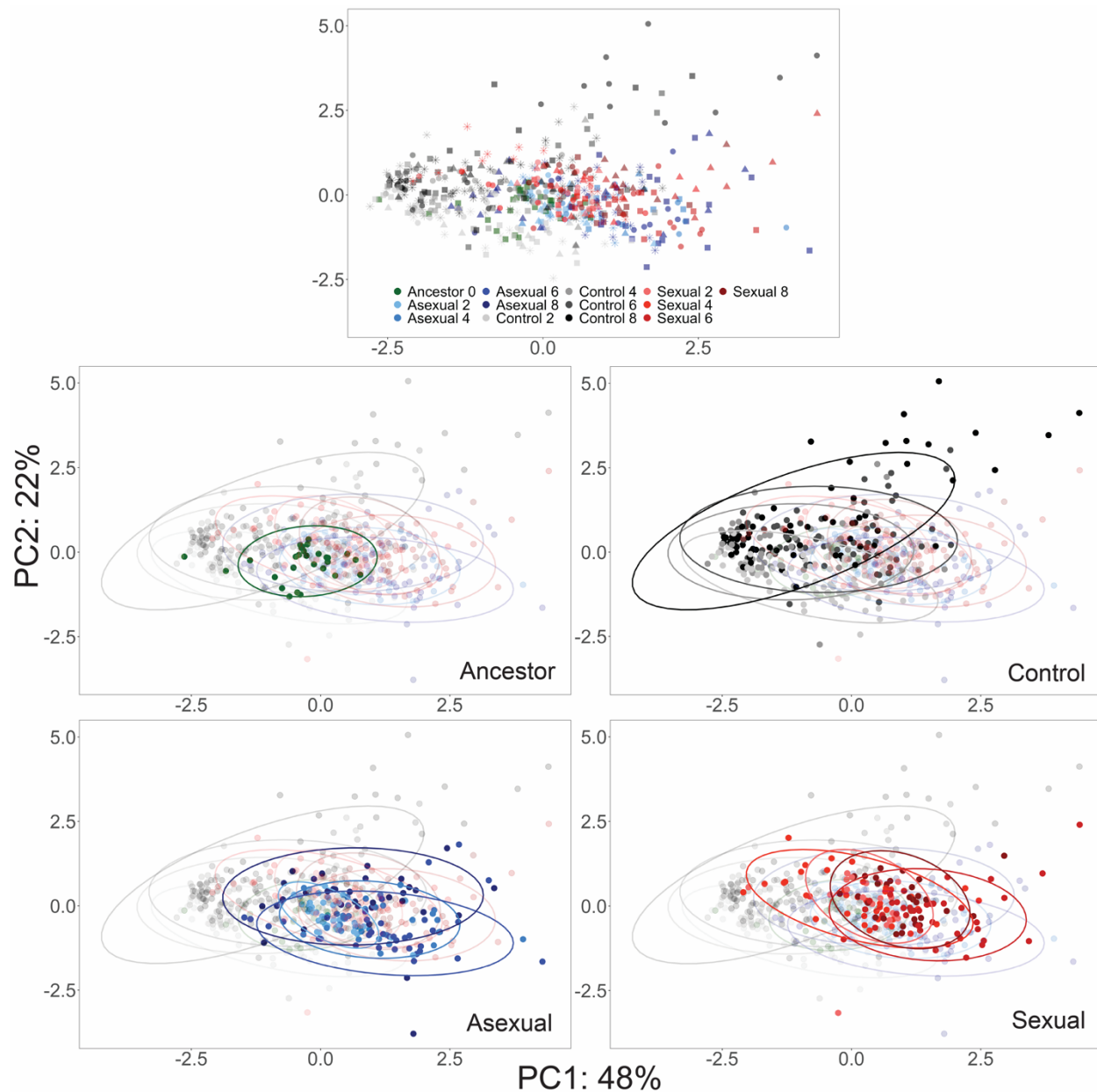774 populations.
775

Figure S5: PCA of YJM128 Evolved Populations.
Each point represents a single clone; ancestor- green, control- gray through black, asexual- light blue through dark blue, sexual- light red through dark red. Colors become darker as cycle number increases. In the first panel, shapes as in Figure 4 to highlight different replicate populations.
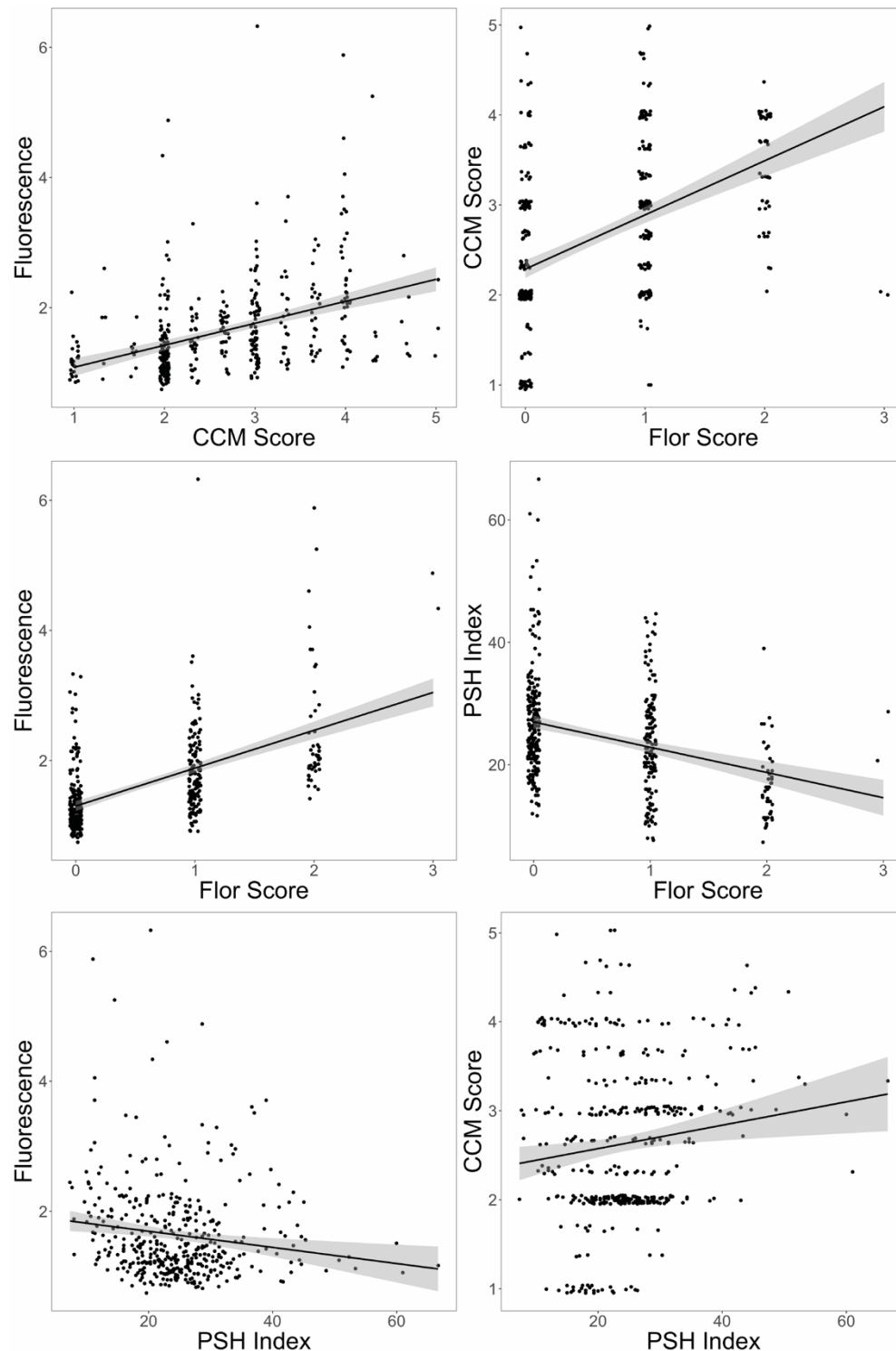
782
783 **Figure S6: Correlations among phenotypes for individual clones from YJM311**
784 **populations.** All correlations were significant with $p < 0.001$. The adjusted R^2 for the
785 relationships are as follows: PA vs. CCM: 0.167, PA vs. Flor: 0.306, PA vs. PSH: 0.020, CCM
786 vs. Flor: 0.220, PSH vs Flor: 0.105, CCM vs. PSH: 0.015. Despite the statistical significance,
787 most of these correlations explain little of the variance in the data; the presence of one
788 multicellular phenotype does not necessarily have predict the presence of another.
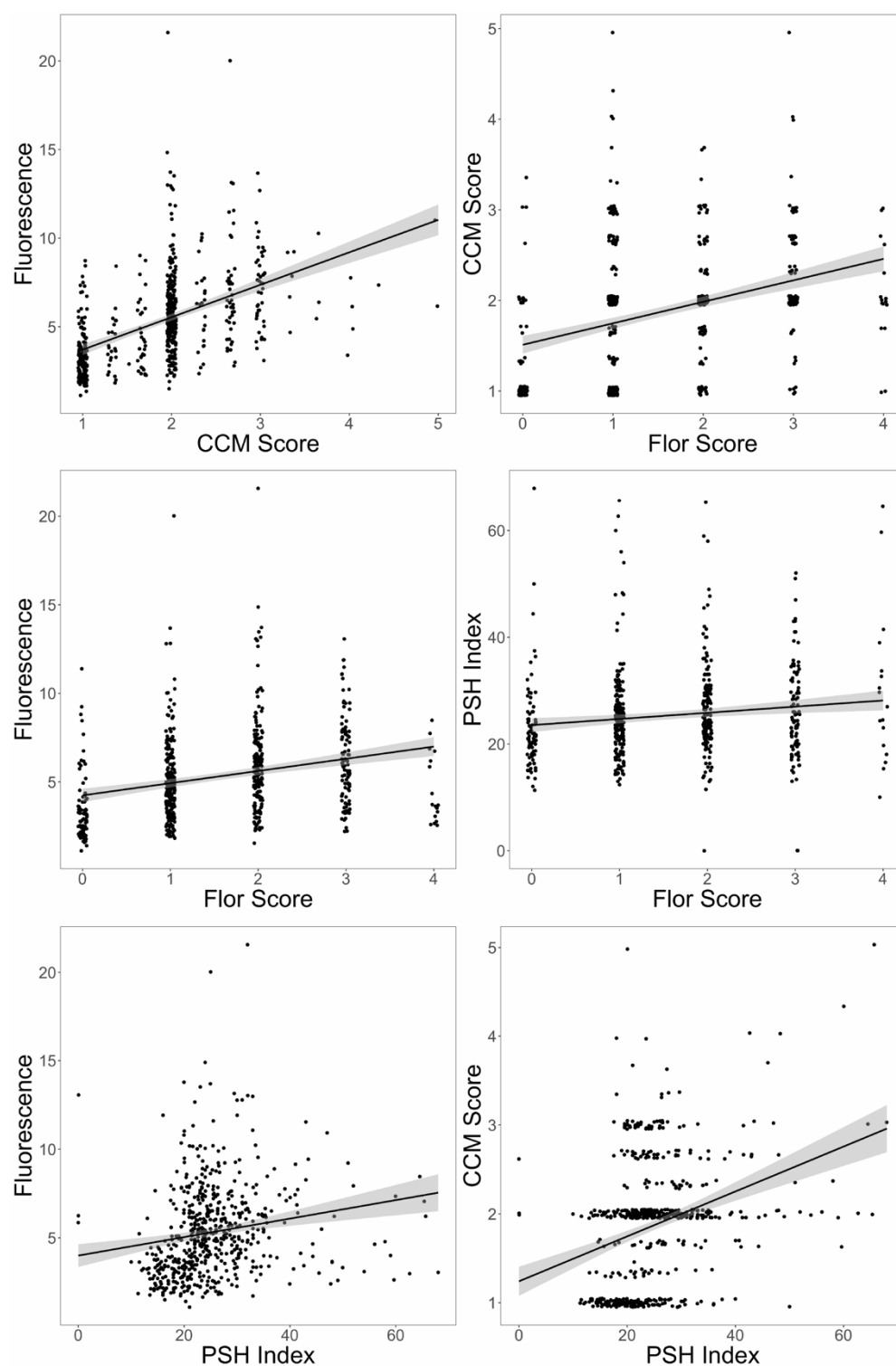
789
Figure S7: Correlations among phenotypes for individual clones from YJM128 populations. All correlations were significant with $p < 0.001$. The adjusted R^2 for the relationships are as follows: PA vs. CCM: 0.235, PA vs. Flor: 0.071, PA vs. PSH: 0.0294, CCM vs. Flor: 0.121, PSH vs Flor: 0.0162, CCM vs. PSH: 0.102. Despite the statistical significance, most of these correlations explain little of the variance in the data; the presence of one multicellular phenotype does not necessarily predict the presence of another.
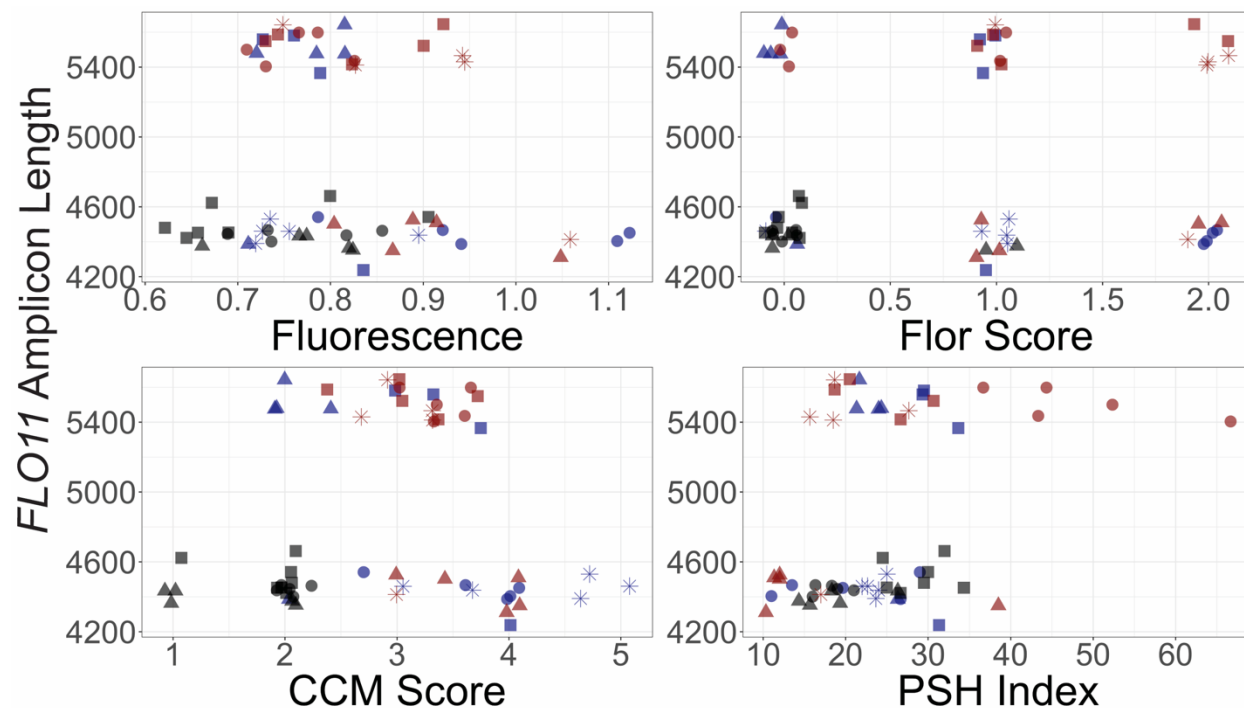
Figure S8: *FLO11* Length by Phenotype for the YJM311 Background.
FLO11 length measurements, point shapes and point colors as in Figure 3. Each panel plots the allele length for a clone with one of its phenotypic measurements.
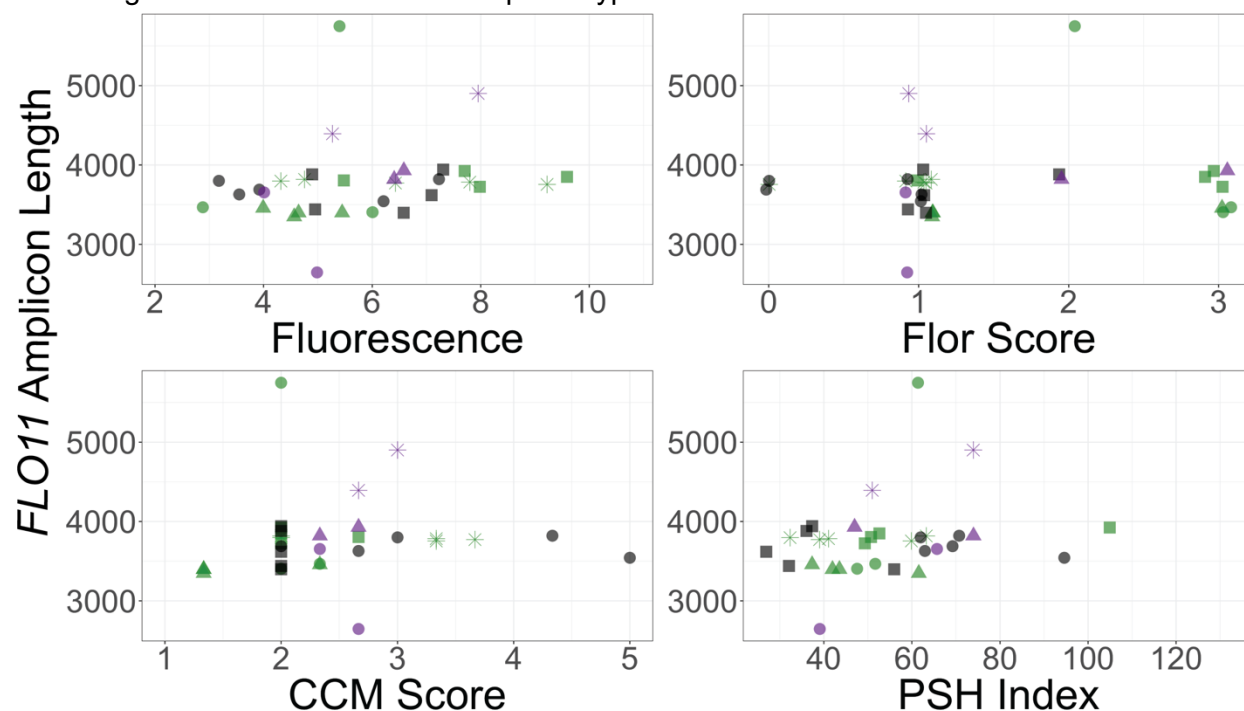

Figure S9: *FLO11* Length by Phenotype for the YJM128 Background.
FLO11 length measurements, point shapes and point colors as in Figure 3. Each panel plots the allele length for a clone with one of its phenotypic measurements.

805 **Figure S10: Survival Assay by Strain.**
806 Data as in Figure 4. Information on individual strains can be found in Tables S1 and S2.